

OPTIMAL POLYNOMIAL SMOOTHERS FOR PARALLEL AMG*

PASQUA D'AMBRA[†], FABIO DURASTANTE[‡], SALVATORE FILIPPONE[§], STEFANO MASSEI[¶], AND STEPHEN THOMAS^{||}

Abstract. In this paper we propose some Chebyshev polynomials of the 1st-kind which produce optimal bound for a polynomial dependent constant involved in the AMG V -cycle error bound and do not require information about the spectrum of matrices. We formulate a variant of a minimax problem already proposed in [J. LOTTES, *Optimal polynomial smoothers for multigrid V -cycles*, Numer. Lin. Alg. with Appl., 30 (2023), p. e2518, <https://doi.org/10.1002/nla.2518>] and define Chebyshev polynomial of the 1st-kind as acceleration for a weighted-Jacobi smoother; we also describe efficient GPU kernels for the application of the polynomial smoother and compare results with accelerators defined in [J. LOTTES, *Optimal polynomial smoothers for multigrid V -cycles*, Numer. Lin. Alg. with Appl., 30 (2023), p. e2518, <https://doi.org/10.1002/nla.2518>] on usual benchmarks at very large scales.

Key words. AMG, parallel smoothers, Chebyshev polynomials, GPU

MSC codes. 65F10, 65F08, 65N55, 65Y05

1. Introduction. Algebraic MultiGrid (AMG) methods are optimal iterative solvers for a large class of linear systems, particularly effective for those arising from scalar elliptic isotropic Partial Differential Equations (PDEs), achieving near-constant iteration counts regardless of the problem size [24, 25]. This property, known as *algorithmic scalability*, combined with optimal linear-time complexity, makes AMG methods highly suitable for the exascale computing challenge [2].

Traditionally, the Gauss-Seidel method is the preferred smoother for AMG, often implemented in a parallel hybrid variant using block-Jacobi iterations [3]. However, this approach can degrade the smoothing properties and is inefficient on modern multi/many-core processors; hence research has focused on finding smoothers that work well in this context [1, 3, 7, 15]. Polynomial smoothers offer an alternative, leveraging sparse matrix-vector products, which are well-optimized on contemporary

*This work was partially supported by: Spoke 1 “FutureHPC & BigData” and Spoke 6 “Multi-scale Modelling & Engineering Applications” of the Italian Research Center on High-Performance Computing, Big Data and Quantum Computing (ICSC) funded by MUR Missione 4 Componente 2 Investimento 1.4: Potenziamento strutture di ricerca e creazione di “campioni nazionali di R&S (M4C2-19)” - Next Generation EU (NGEU); the “Energy Oriented Center of Excellence (EoCoE III): Fostering the European Energy Transition with Exascale” EuroHPC Project N. 101144014, funded by European Commission (EC); the “INdAM-GNCS Project: Metodi basati su matrici e tensori strutturati per problemi di algebra lineare di grandi dimensioni”, CUP E53C22001930001; the European Union - NextGenerationEU under the National Recovery and Resilience Plan (PNRR) - Mission 4 Education and research - Component 2 from research to business - Investment 1.1 Notice Prin 2022 - DD N. 104 2/2/2022, titled “Low-rank Structures and Numerical Methods in Matrix and Tensor Computations and their Application”, proposal code 20227PCCKZ – CUP I53D23002280006. FD and SM acknowledge the MIUR Excellence Department Project awarded to the Department of Mathematics, University of Pisa, CUP I57G22000700001. PD, FD and SF are members of INdAM-GNCS.

[†]Istituto per le Applicazioni del Calcolo “Mauro Picone”, Consiglio Nazionale delle Ricerche, Via Pietro Castellino, 111, Naples 80131, Italy (pasqua.dambra@cnr.it).

[‡]Dipartimento di Matematica, Università di Pisa, Largo Bruno Pontecorvo, 5, Pisa 56127, Italy (fabio.durastante@unipi.it, fdurastante.github.io).

[§]Dipartimento di Ingegneria Civile e Ingegneria informatica, Università di Roma “Tor Vergata”, Via del Politecnico, 1, Rome 00133, Italy. (salvatore.filippone@uniroma2.it)

[¶]Dipartimento di Matematica, Università di Pisa, Largo Bruno Pontecorvo, 5, Pisa 56127, Italy (stefano.massei@unipi.it).

^{||}Advanced Micro Devices, HPC and DC-GPU, Austin TX, USA. (stephen.thomas2@amd.com)

hardware. This paper deals with the usage of polynomial smoothers within AMG to solve symmetric positive definite (SPD) linear systems:

$$(1.1) \quad A\mathbf{x} = \mathbf{b}, \quad \text{with } A \in \mathbb{R}^{n \times n} \text{ SPD and } \mathbf{x}, \mathbf{b} \in \mathbb{R}^n.$$

The selection of polynomial smoothers, their degrees, and related parameters, significantly impact AMG performance. Lottes [18] recently provided convergence analysis for AMG's two-level and V -cycle formulations, where error bounds depend on polynomial acceleration. This allows for strategies optimizing the convergence constant for the V -cycle, a method previously used in geometric multigrid for unsteady flow problems [4, 5, 6, 17]. Our focus is on Chebyshev-type polynomial smoothers [1, 18], which optimize the two-level energy-norm error propagation matrix. Additionally, we aim to develop smoothers and optimization procedures independent of the matrix spectrum, unlike those discussed in [3, 12, 16, 22].

This paper introduces, a minimax problem variant for optimizing the V -cycle error bound, building on Lottes' work [18]. We employ 1st-kind Chebyshev polynomials on a suitable interval $[a^*, 1]$, optimizing the left endpoint by solving a non-linear equation varying the polynomial degree. These polynomials achieve lower V -cycle error bounds for low-degree polynomials ($k \leq 5$) compared to Lottes' 4th-kind Chebyshev polynomials and are comparable to the numerically-approximated optimal bounds [18]. We have also developed efficient NVIDIA GPU kernels for these polynomial accelerators within the Parallel Sparse Computation Toolkit (PSCToolkit) framework [9], demonstrating the benefits on large-scale benchmarks.

The paper is organized as follows: Section 2 outlines the construction of polynomial smoothers and our proposal, Section 3 details the AMG method construction using AMG4PSBLAS [8] from the PSCToolkit suite [9]. Section 4 discusses GPU implementation details and benchmark tests. Finally, Section 5 concludes and suggests future research directions.

2. Polynomial Smoothers for AMG. We start by briefly recalling the expression for a stationary iteration, representing a generic AMG method for the symmetric and positive definite A in (1.1)

$$\mathbf{x}^{(k)} = \mathbf{x}^{(k-1)} + B \left(\mathbf{b} - A\mathbf{x}^{(k-1)} \right), \quad k = 1, 2, \dots \quad \text{given } \mathbf{x}^{(0)} \in \mathbb{R}^n,$$

where the matrix B can be defined recursively by composing a coarse grid correction together with a simple fixed point iteration. Specifically, let A_l be a sequence of coarse matrices computed by the triple-matrix Galerkin product:

$$A_{l+1} = P_l^T A_l P_l, \quad l = 0, \dots, N_l - 1,$$

with $A_0 = A$ and P_l a sequence of prolongation matrices of size $n_l \times n_{l+1}$, with $n_{l+1} < n_l$ and $n_0 = n$. Then we can take any iteration matrix M_l that is an A_l -convergent smoother for A_l , i.e., $\|I - M_l^{-1}A_l\|_{A_l} < 1$, where I is the identity matrix of size n_l and $\|\cdot\|_{A_l}$ indicates the A_l -energy-norm, and construct B as the multiplicative composition of the following error propagation matrices:

$$(2.1) \quad I - B_l A_l = (I - M_l^{-T} A_l)^k (I - P_l B_{l+1} P_l^T A_l) (I - M_l^{-1} A_l)^k \quad \forall l < N_l, k \geq 1,$$

where we are assuming that the coarsest A_l is solved by a direct method.

Instead of the smoothing iteration:

$$G = (I - M_l^{-1} A_l)^k, \quad k \geq 1,$$

we want to consider polynomial iterations of the form:

$$G = p_k(M_l^{-1}A_l), \quad p_k(x) \in \Pi_k,$$

for the set of polynomials Π_k defined as

$$(2.2) \quad \Pi_k = \{p \text{ polynomial of degree at most } k : p(0) = 1, \quad |p(x)| \leq 1 \quad \forall x \in [0, 1]\}.$$

If we restrict the analysis to the case in which we employ only two levels, we can drop the l index, and let $P \in \mathbb{R}^{n \times n_c}$ be the prolongator from the fine to the coarse space and $A_c = P^T A P$ be the Galerkin coarse matrix. Then the error propagation matrix for the two-level symmetric V -cycle, when k iterations of the smoother are applied before and after the coarse-space correction in (2.1) can be compactly rewritten as:

$$E = G^T (I - P A_c^{-1} P^T A) G.$$

The following bound can be obtained:

$$(2.3) \quad \|E\|_A^2 \leq \frac{C}{C + 2k},$$

where C is the following approximation property constant:

$$(2.4) \quad C = \|A^{-1} - P A_c^{-1} P^T\|_{A,B}^2 = \sup_{\|u\|_B \leq 1} \|(A^{-1} - P A_c^{-1} P^T)u\|_A^2,$$

that is an approximation property of the vectors in $\mathbb{R}^{n \times n}$ by vectors from the subspace $\mathbb{R}^{n_c \times n_c}$; see, e.g., [20, Theorem 3.4]. If we now go back to considering all the levels, it follows that the resulting convergence estimate for (2.1) is given by the largest of (2.3) at the various levels [14, Theorem 4.5]. The previous analysis can be refined for the case of a generic polynomial smoother as follows.

PROPOSITION 2.1 ([18, Lemma 2]). *Let the smoother iteration (on each level) be represented by:*

$$G_l = p^l(M^{-1}A),$$

where $p^l(x)$ is a polynomial satisfying $p^l(0) = 1$ and $|p^l(x)| < 1$ for $0 < x \leq 1$, possibly different on each level. Then the V -cycle error propagation matrix satisfies the following bound:

$$(2.5) \quad \|E\|_A^2 \leq \max_l \frac{C_l}{C_l + \gamma_l^{-1}},$$

where C_l is the approximation property constant in (2.4) at the level l and

$$\gamma_l = \sup_{0 < \lambda \leq 1} \frac{\lambda p^l(\lambda)^2}{1 - p^l(\lambda)^2}.$$

The analysis and construction of the smoothers that we deal with in this paper is therefore based on the search for polynomials attempting to optimize the above convergence bound.

Having observed this behavior on the levels and focusing on the choice of the smoother, we now drop the level indication—the l subscript—and generally assume that we are using the same smoother at all levels of the V -cycle (2.1), i.e., we set

$p^l(x) = p_k(x) \in \Pi_k[x]$ for all l . Furthermore, because our use case for these polynomial smoothers is that of a Single Instruction/Multiple Data (SIMD) computing environment—a GPU accelerator, or a multi-thread acceleration—we further focus our attention on a smoother that can be applied efficiently in this context such as the ℓ_1 -Jacobi smoother:

$$(2.6) \quad G = M^{-1}N = I - M^{-1}A, \quad \begin{aligned} M &= \text{diag}(M_{ii})_{i=1,\dots,n}, \\ M_{ii} &= a_{ii} + \sum_{j \neq i} |a_{ij}|, \end{aligned} \quad A = M - N.$$

Polynomial acceleration of such methods is a classic topic [13] about which we report again only briefly the idea. For any fixed-point iterative method of the form

$$\mathbf{x}^{(k+1)} = \mathbf{x}^{(k)} + M^{-1}(\mathbf{b} - A\mathbf{x}^{(k)}) = M^{-1}(N\mathbf{x}^{(k)} + \mathbf{b}), \quad k \geq 0, \quad A = M - N,$$

we have seen that the error can be expressed as

$$\mathbf{e}^{(k+1)} = \mathbf{x}^{(k+1)} - \mathbf{x} = M^{-1}N(\mathbf{x}^{(k)} - \mathbf{x}) = M^{-1}N\mathbf{e}^{(k)}.$$

We would like to construct an accelerated sequence based upon the linear combination

$$(2.7) \quad \mathbf{y}^{(k)} = \sum_{j=0}^k \nu_{j,k} \mathbf{x}^{(j)}, \quad \sum_{j=0}^k \nu_{j,k} = 1,$$

that is used in conjunction with the error equation; this would give us

$$\begin{aligned} \sum_{j=0}^k \nu_{j,k} (\mathbf{x}^{(j)} - \mathbf{x}) &= \sum_{j=0}^k \nu_{j,k} (M^{-1}N)^j \mathbf{e}^{(0)} = \tilde{p}_k(M^{-1}N) \mathbf{e}^{(0)} \\ &= \tilde{p}_k(I - M^{-1}A) \mathbf{e}^{(0)} = p_k(M^{-1}A) \mathbf{e}^{(0)}. \end{aligned}$$

However this approach is not convenient on the implementation side, as it would require storing and summing k vectors for each application. The most efficient procedure takes advantage of the short-term recurrences of the prescribed family of polynomials; see Section 2.1 and Section 2.2.

To optimize the bound in Proposition 2.1 we then have to solve the minimax problem

$$(2.8) \quad \gamma_k := \min_{p(x) \in \Pi_k} \max_{x \in (0,1]} \left| \frac{xp(x)^2}{1-p(x)^2} \right|$$

with the set Π_k as in (2.2).

This is indeed different from the energy norms of the residual $\|\mathbf{r}\|_A$ and error $\|\mathbf{e}\|_A$ that are optimized in the derivation of (preconditioned) Krylov methods for symmetric matrices A , such as conjugate gradients.

In the remainder of the section we will focus on determining polynomials that (approximately) solve (2.8) and building the corresponding application routines.

2.1. 4th-kind Chebyshev polynomials. In order to make a comparison, we describe the approach discussed in [18] based upon the 4th-kind Chebyshev polynomials:

$$W_k(x) = \frac{\cos(k + 1/2)\theta}{\cos(\theta/2)}, \quad n \geq 0, \quad x = \cos(\theta),$$

whose choice produces the following polynomial smoother, expressed as a simple three-terms recurrence:

$$\begin{aligned}
 \mathbf{z}^{(0)} &= \mathbf{0}, \\
 \mathbf{r}^{(0)} &= \mathbf{b} - A\mathbf{x}^{(0)}, \\
 \mathbf{x}^{(k)} &= \mathbf{x}^{(k-1)} + \mathbf{z}^{(k)}, \\
 \mathbf{z}^{(k)} &= \frac{2k-3}{2k+1}\mathbf{z}^{(k-1)} + \frac{8k-4}{2k+1}\frac{1}{\rho(M^{-1}A)}M^{-1}\mathbf{r}^{(k-1)} \\
 \mathbf{r}^{(k)} &= \mathbf{r}^{(k-1)} - A\mathbf{z}^{(k)}.
 \end{aligned}
 \tag{2.9}$$

If M is an spd smoother, then using Proposition 2.1, the polynomial smoother (2.9) produces an error propagation matrix of the symmetric multilevel V -cycle (2.1) obeying the following bound:

$$\|E\|_A^2 \leq \max_{l=1,\dots,N_l-1} \frac{C_l}{C_l + 4/3k_l(k_l + 1)},
 \tag{2.10}$$

where C_l is the approximation property constant and k_l is the polynomial degree at the level l .

The other approach employed in [18] is to solve numerically for the optimal polynomial $p(x)$ in (2.8) by applying Newton's method to a system of nonlinear equations expressing the equi-oscillation property, and then write:

$$p_k(x) = \sum_{j=0}^k \frac{\beta_{j,k} - \beta_{j+1,k}}{2j+1} W_j(1-2x), \quad \beta_{0,k} = 1, \quad \beta_{k+1,k} = 0 \quad \forall k \geq 0.$$

By this choice we can modify the update of the $\mathbf{x}^{(k)}$ vector in (2.9) with

$$\mathbf{x}^{(k)} = \mathbf{x}^{(k-1)} + \beta_k \mathbf{z}^{(k)},
 \tag{2.11}$$

taking care to always compute the residual with respect to the original solution, i.e., not multiplying by the factor β_k in its update; see [18] for further comments. In Fig. 1 we report on the two different choices of polynomials. The β_k coefficients are obtained by the Gaussian quadrature rule applied to the orthogonality relation for the 4th-kind Chebyshev polynomials W_j .

We observe that application of the above smoother, for a polynomial degree k , requires k applications of the basic smoother to the residual vector, two vector operations (**axpy**) for updating vectors z and x , and one sparse matrix-vector product (**SpMV**) plus another **axpy** for updating the residual. Therefore, the smoother application requires k **axpy** operations more than k iterations of the basic smoother; we will deal with the efficient GPU implementation of the procedure in Section 3.

2.2. Accelerated sequence with optimal 1st-kind Chebyshev polynomials. We describe here the procedure for applying the 1st-kind Chebyshev polynomial acceleration that we propose as smoother. Let us recall that the Chebyshev polynomials of the 1st-kind are the family of orthogonal polynomials on the interval $[-1, 1]$ with respect to the inner product $\langle h, g \rangle = \int_{-1}^1 h(x)g(x)\frac{dx}{\sqrt{1-x^2}}$. Let $\tau_k(x)$ denote the polynomial of degree k ; we have $\tau_0(x) = 1$, $\tau_1(x) = 2x$, and higher degree polynomials can be computed via the recurrence relation $\tau_{k+1}(x) = 2x \cdot \tau_k(x) - \tau_{k-1}(x)$.

Chebyshev polynomials can be generalized to an arbitrary compact real interval $[a, b] \subset \mathbb{R}$, in the sense of constructing the polynomials $\tau_k^{[a,b]}(x)$ that are monic and

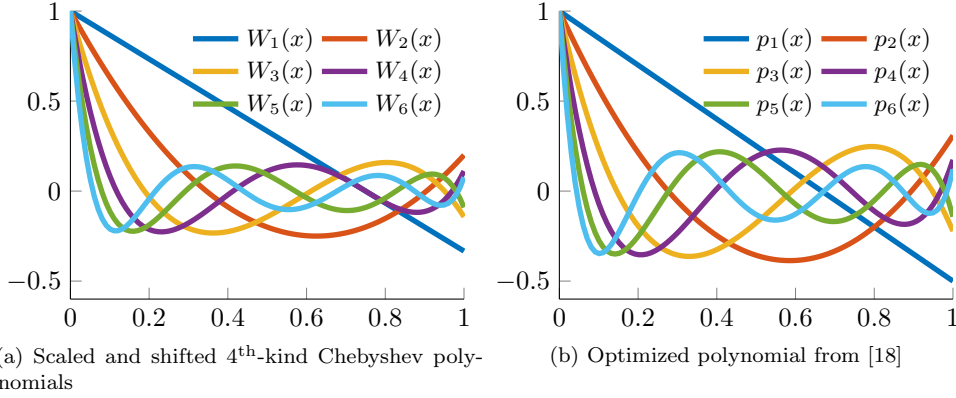


Fig. 1: Polynomials for accelerating the fixed point iterative method to use as a smoother from [18]. The left panel contains the standard 4th-kind Chebyshev polynomials, the right panel has the polynomials computed by numerically solving the system of nonlinear equations respecting the equi-oscillation property and optimizing the bound in Proposition 2.1.

orthogonal with respect to the inner product $\langle h, g \rangle = \int_a^b h(x)g(x) \frac{dx}{\sqrt{(a-x)(b-x)}}$. This can be done by composing τ_k with a linear map from $[a, b]$ to $[-1, 1]$ and by applying a scaling:

$$\tau_k^{[a,b]}(x) = \tau_k \left(\frac{b+a}{b-a} - \frac{2x}{b-a} \right) / \tau_k \left(\frac{b+a}{b-a} \right).$$

We remark that the scaling is not necessary for the orthogonality but it ensures the normalization property $\tau_k^{[a,b]}(0) = 1$. The corresponding recurrence relation is then given by

$$(2.12) \quad \begin{aligned} \tau_0^{[a,b]}(x) &= 1, \\ \tau_1^{[a,b]}(x) &= 1 - \frac{2x}{b+a}, \\ \tau_{k+1}^{[a,b]}(x) &= \frac{\tau_k(\frac{b+a}{b-a})}{\tau_{k+1}(\frac{b+a}{b-a})} \left[2 \left(\frac{b+a}{b-a} - \frac{2x}{b-a} \right) \tau_k^{[a,b]}(x) - \frac{\tau_{k-1}(\frac{b+a}{b-a})}{\tau_k(\frac{b+a}{b-a})} \tau_{k-1}^{[a,b]}(x) \right]. \end{aligned}$$

Since we plan to optimize over the a parameter, having b set to 1, we pose

$$(2.13) \quad \theta = \frac{1+a}{2}, \quad \delta = \frac{1-a}{2},$$

and rewrite (2.12) over a centered interval as

$$(2.14) \quad \begin{aligned} \tau_0^{[a,1]}(x) &= 1, \\ \tau_1^{[a,1]}(x) &= 1 - \frac{x}{\theta}, \\ \tau_{k+1}^{[a,1]}(x) &= \frac{\sigma_k}{\sigma_{k+1}} \left[2 \frac{\theta-x}{\delta} \tau_k^{[a,1]}(x) - \frac{\sigma_{k-1}}{\sigma_k} \tau_{k-1}^{[a,1]}(x) \right], \quad k \geq 1. \end{aligned}$$

with the normalization constants given by

$$\sigma_0 = 1,$$

$$\begin{aligned}\sigma_1 &= \frac{\theta}{\delta}, \\ \sigma_{k+1} &= 2\frac{\theta}{\delta}\sigma_k - \sigma_{k-1}, \quad k \geq 1.\end{aligned}$$

The Chebyshev acceleration for the fixed point iteration is then summarized in the following recurrence:

$$\begin{aligned}(2.15) \quad \mathbf{r}^{(0)} &= \frac{1}{\rho(M^{-1}A)} M^{-1}(\mathbf{b} - A\mathbf{x}^{(0)}) \\ \mathbf{z}^{(0)} &= \frac{2}{1+a}\mathbf{r}^{(0)}, \quad \rho_0 = \frac{1-a}{1+a} \\ \rho_k &= \left(\frac{2(1+a)}{1-a} - \rho_{k-1}\right)^{-1} \\ \mathbf{x}^{(k)} &= \mathbf{x}^{(k-1)} + \mathbf{z}^{(k-1)} \\ \mathbf{r}^{(k)} &= \mathbf{r}^{(k-1)} - \frac{1}{\rho(M^{-1}A)} M^{-1}A\mathbf{z}^{(k-1)} \\ \mathbf{z}^{(k)} &= \rho_k \rho_{k-1} \mathbf{z}^{(k-1)} + \frac{4\rho_k}{(1-a)} \mathbf{r}^{(k)}\end{aligned}$$

The above acceleration guarantees that the error at step k behaves as

$$\mathbf{e}^{(k)} = \mathbf{x}^{(k)} - \mathbf{x} = \tau_k^{[a,1]} (\rho^{-1}(M^{-1}A) M^{-1}A) \mathbf{e}^{(0)},$$

for any value of the a parameter. This is the analogue of the formulas (2.11) for the polynomial acceleration based on the Chebyshev polynomials of the 4th-kind for the smoother in (2.6).

We observe that the application of the above smoother, for a polynomial of degree k , has the same cost of the smoother based on the 4th-kind Chebyshev polynomial, as it requires k applications of the basic smoother, k SpMV for updating the residual vector, and two vector operations (**axpy**) for updating d and x ; again, we postpone the discussion of an efficient GPU implementation of the procedure to Section 3. In the next Section 2.3, we will address the choice of a according to the convergence analysis outlined in Proposition 2.1.

2.3. Revisiting the polynomial optimization problem. Herein, we propose an alternative family of polynomials which provides a quasi-optimal solution for the minimax problem in (2.5). We start by rewriting problem (2.8) as

$$\gamma_k = \min_{p(x) \in \Pi_k} \max_{x \in (0,1]} x \left| 1 - \frac{1}{1 - p(x)^2} \right|,$$

i.e., we can consider this as a search for the most favorable minimax approximation relative to an unconventional weight, targeting the zero function across the interval $(0, 1]$ over the set of monic polynomials of degree bounded by k . The latter constraint is indeed what makes the issue non trivial as each candidate solution has to pass through 1 at $x = 0$.

The core idea of this section is to analyze the values of the objective function when restricting to the set of scaled 1st-kind Chebyshev polynomials. The motivation for this is that those polynomials would provide the optimal solution whenever we replace the weight function with 1 and the interval $(0, 1]$ with $[a, 1]$, for any $a \in (0, 1)$.

2.3.1. 1st-kind Chebyshev polynomials: basic properties. We report here some well known results about Chebyshev polynomials that will be needed in the subsequent analysis. We refer to [19, Chapter 1] for the basic properties and functional identities, while we point to [19, Chapter 3] for the minimax approximation properties.

(i) For $x \in \mathbb{R}$, $\tau_k(x)$ verifies the following identity

$$\tau_k(x) = \frac{1}{2} \left[(x + \sqrt{x^2 - 1})^k + (x - \sqrt{x^2 - 1})^k \right].$$

(ii) The polynomial $\tau_k^{[a,b]}(x)$ is the monic polynomial of degree at most k that deviates least from 0 on $[a, b]$. More precisely, $\tau_k^{[a,b]}(x)$ solves the optimization problem

$$\tau_k^{[a,b]}(x) = \arg \min_{\{\deg(p)=k, p(0)=1\}} \max_{x \in [a,b]} |p(x)|,$$

and the associated optimal value verifies

$$\max_{x \in [a,b]} |\tau_k^{[a,b]}(x)| = 2 \left[\left(\frac{\sqrt{\kappa} - 1}{\sqrt{\kappa} + 1} \right)^k + \left(\frac{\sqrt{\kappa} + 1}{\sqrt{\kappa} - 1} \right)^k \right]^{-1} \leq 2 \left(\frac{\sqrt{\kappa} - 1}{\sqrt{\kappa} + 1} \right)^k,$$

where $\kappa = \frac{b}{a}$.

(iii) The zeros of $\tau_k^{[a,b]}$, and of $\frac{d}{dx}(\tau_k^{[a,b]})$ are inside $[a, b]$. Combining this with $\tau_k^{[a,b]}(0) = 1$, and $|\tau_k^{[a,b]}| \leq 1$ in $[a, b]$, implies that $\tau_k^{[a,b]}$ is decreasing in $[0, a]$. In particular, when $b = 1$ we have $\tau_k^{[a,1]} \in \Pi_k$.

2.3.2. Restricting the problem to the 1st-kind Chebyshev polynomials of degree k . To get a computable upper bound for the optimal value γ_k of (2.8), we restrict the set of feasible polynomials to $\mathcal{C}_k := \{\tau_k^{[a,1]}, a \in [0, 1)\} \subset \Pi_k$ and we consider

$$(2.16) \quad \Lambda_k := \min_{p(x) \in \mathcal{C}_k} \max_{x \in (0,1]} x \left| 1 - \frac{1}{1 - p(x)^2} \right| = \min_{a \in [0,1)} \max_{x \in (0,1]} x \left| 1 - \frac{1}{1 - \tau_k^{[a,1]}(x)^2} \right|.$$

Since the Chebyshev polynomial $\tau_k^{[a,1]}(x)$ has very different behaviours inside and outside the interval $[a, 1]$ it is convenient to divide the analysis of the minimax problem in two parts: one related to the half open interval $(0, a]$ and the other to the closed interval $[a, 1]$. Formally, we use that

$$(2.17) \quad \sup_{x \in (0,1]} x \left| 1 - \frac{1}{1 - \tau_k^{[a,1]}(x)^2} \right| = \max \left\{ \sup_{x \in (0,a]} \frac{x \tau_k^{[a,1]}(x)^2}{1 - \tau_k^{[a,1]}(x)^2}, \max_{x \in [a,1]} \frac{x \tau_k^{[a,1]}(x)^2}{1 - \tau_k^{[a,1]}(x)^2} \right\}.$$

The first step is showing that, whenever we fix a polynomial in \mathcal{C}_k , the objective function in the max problem is positive and monotonically decreasing on $(0, a]$; since the proof of this is rather technical, it is moved to Appendix A.

LEMMA 2.2. *The function $f(x) := \frac{x \tau_k^{[a,1]}(x)^2}{1 - \tau_k^{[a,1]}(x)^2}$ is positive and monotonically decreasing on $(0, a]$ for any $k \in \mathbb{N}$, and for any $a \in (0, 1)$.*

Let $c_j^{(a,k)}$ denote the coefficient of degree j of $\tau_k^{[a,1]}$; in view of Lemma 2.2, we have

$$\sup_{x \in (0,a]} \frac{x \tau_k^{[a,1]}(x)^2}{1 - \tau_k^{[a,1]}(x)^2} = \lim_{x \rightarrow 0^+} \frac{x \tau_k^{[a,1]}(x)^2}{1 - \tau_k^{[a,1]}(x)^2} = \frac{1}{2|c_1^{(a,k)}|},$$

meaning that the maximum error in $(0, a]$ corresponding to $\tau_k^{[a,b]}$ is $\frac{1}{2|c_1^{(a,k)}|}$ and is equal to the absolute value of the reciprocal of the coefficient of degree one given by $\tau_k^{[a,1]}(x)^2$. Let us provide an explicit formula for $c_1^{(a,k)}$; we have that $c_1^{(a,k)} = [\tau_k^{[a,1]}]'(0)$, and in view of the relation $\tau_k'(x) = kq_{k-1}(x)$, with $q_j(x)$ indicating the j th Chebyshev polynomial of the 2nd-kind, it follows

$$(2.18) \quad c_1^{(a,k)} = -\frac{2k}{1-a} q_{k-1} \left(\frac{1+a}{1-a} \right) / \tau_k \left(\frac{1+a}{1-a} \right).$$

For a real argument x , Chebyshev polynomials of the 2nd-kind can be expressed with the formula

$$q_k(x) = \frac{(x + \sqrt{x^2 - 1})^{k+1} - (x - \sqrt{x^2 - 1})^{k+1}}{2\sqrt{x^2 - 1}}.$$

By substituting the formula for Chebyshev coefficients (both first and second kind) into (2.18), and letting $y = \frac{1+a}{1-a}$ we get

$$\begin{aligned} c_1^{(a,k)} &= -\frac{2k}{1-a} \cdot \frac{(y + \sqrt{y^2 - 1})^k - (y - \sqrt{y^2 - 1})^k}{(y + \sqrt{y^2 - 1})^k + (y - \sqrt{y^2 - 1})^k} \cdot \frac{1}{\sqrt{y^2 - 1}} \\ &= -\frac{2k}{1-a} \cdot \left[1 - \frac{2(y - \sqrt{y^2 - 1})^k}{(y + \sqrt{y^2 - 1})^k + (y - \sqrt{y^2 - 1})^k} \right] \cdot \frac{1}{\sqrt{y^2 - 1}} \\ &= -\frac{2k}{1-a} \cdot \left[1 - \frac{2}{(y + \sqrt{y^2 - 1})^{2k} + 1} \right] \cdot \frac{1}{\sqrt{y^2 - 1}} \\ &= -\frac{2k}{1-a} \cdot \left[1 - \frac{2}{\left(\frac{1+\sqrt{a}}{1-a}\right)^{2k} + 1} \right] \cdot \frac{1-a}{2\sqrt{a}} \\ &= -\frac{k}{\sqrt{a}} \left[1 - \frac{2(1-a)^{2k}}{(1+\sqrt{a})^{4k} + (1-a)^{2k}} \right] \\ &= -\frac{k}{\sqrt{a}} \cdot \frac{(1+\sqrt{a})^{2k} - (1-\sqrt{a})^{2k}}{(1+\sqrt{a})^{2k} + (1-\sqrt{a})^{2k}} \\ &= -k \cdot \frac{\sum_{j=0}^{k-1} \binom{2k}{2j+1} a^j}{\sum_{j=0}^k \binom{2k}{2j} a^j} \\ &\Rightarrow \frac{1}{2|c_1^{(a,k)}|} = \frac{\sum_{j=0}^k \binom{2k}{2j} a^j}{2k \sum_{j=0}^{k-1} \binom{2k}{2j+1} a^j}. \end{aligned}$$

The next natural question is about the dependency of $1/2|c_1^{(a,k)}|$ on the parameter a ; the following lemma, that is proven in Appendix A, ensures that such a value is monotonically increasing with respect to a .

LEMMA 2.3. *The function*

$$g(x) := \frac{\sum_{j=0}^k \binom{2k}{2j} x^j}{2k \sum_{j=0}^{k-1} \binom{2k}{2j+1} x^j}$$

is increasing on $(0, 1)$.

Finally, we analyze the objective function in the interval $[a, 1]$. Focusing on the expression $\max_{x \in [a, 1]} x \left| 1 - \frac{1}{1 - \tau_k^{[a, 1]}(x)^2} \right|$, it becomes readily apparent that the maximum is achieved when $x = 1$, at which point the value is given by:

$$\begin{aligned} \frac{\tau_k^{[a, 1]}(1)^2}{1 - \tau_k^{[a, 1]}(1)^2} &= \frac{1}{\tau_k \left(\frac{1+a}{1-a} \right)^2 - 1} \\ &= \frac{1}{\frac{1}{4} \left[\left(\frac{(1+\sqrt{a})^2}{1-a} \right)^k + \left(\frac{(1-\sqrt{a})^2}{1-a} \right)^k \right]^2 - 1} \\ &= \frac{4}{\left[\left(\frac{1+\sqrt{a}}{1-\sqrt{a}} \right)^k + \left(\frac{1-\sqrt{a}}{1+\sqrt{a}} \right)^k \right]^2 - 4}. \end{aligned}$$

Looking back at (2.17), we see that, for a fixed a , we are taking the maximum between two quantities that depend monotonically on a . In particular, $\frac{\tau_k^{[a, 1]}(a)^2}{1 - \tau_k^{[a, 1]}(a)^2}$ decreases from $+\infty$ to 0 on $(0, 1)$ while $\frac{1}{2|c_1^{(a, k)}|}$ is non negative and monotonically increasing in view of Lemma 2.3.

Therefore, there is only one value a_k^* in $(0, 1)$ of the parameter a that satisfies the identity $\frac{1}{2|c_1^{(a, k)}|} = \frac{\tau_k^{[a, 1]}(1)^2}{1 - \tau_k^{[a, 1]}(1)^2}$, i.e.:

$$\frac{\sqrt{a}}{2k} \cdot \frac{(1 + \sqrt{a})^{2k} + (1 - \sqrt{a})^{2k}}{(1 + \sqrt{a})^{2k} - (1 - \sqrt{a})^{2k}} = \frac{4}{\left[\left(\frac{1+\sqrt{a}}{1-\sqrt{a}} \right)^k + \left(\frac{1-\sqrt{a}}{1+\sqrt{a}} \right)^k \right]^2 - 4},$$

and a_k^* is the optimal choice for (2.16); see Fig. 2 in which we show the behaviour of the objective function for different values of a .

By applying some algebraic manipulations to the above equation, we find that $\sqrt{a_k^*}$ is the only root in $(0, 1)$ of the polynomial equation

$$(2.19) \quad 8k(1 - x^2)^{2k} + x \left[(1 - x)^{4k} - (1 + x)^{4k} \right] = 0,$$

that can be approximated by using the combination of bisection, secant, and inverse quadratic interpolation methods available in MATLAB's `fzero` routine and based on the version of Brent's Algorithm from [11].

In Figure 3 we report the first polynomials $\tau_k^{[a, 1]}(x)$ for a the optimal value obtained from the solution of (2.19), that can be compared with the polynomials from Fig. 1.

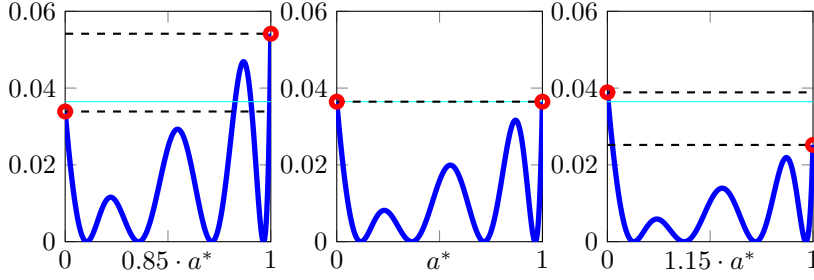


Fig. 2: Graphs of the function $x(\tau_4^{[a,1]}(x))^2 / 1 - (\tau_4^{[a,1]}(x))^2$ for different choices of a , on the left panel $a = 0.85 \cdot a^*$, on the center $a = a^*$, and on the right $a = 1.15 \cdot a^*$ with a^* the optimal value. The solid cyan line “—” represents the optimal value Λ_4 of (2.16).

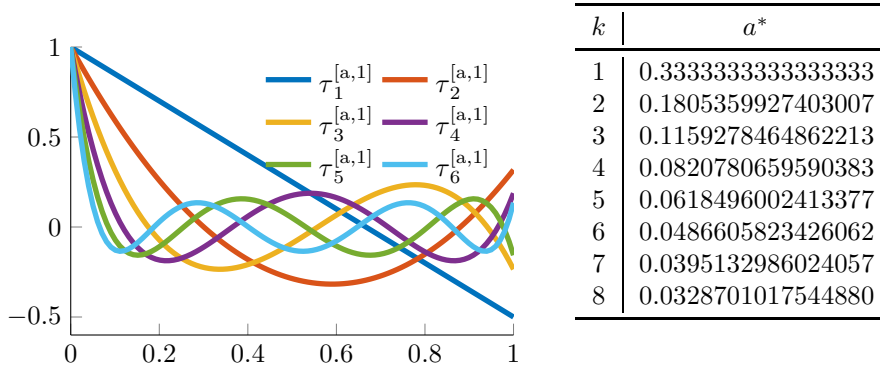


Fig. 3: Optimized shifted and scaled Chebyshev polynomials $\tau_k^{[a^*,1]}(x)$ with a^* computed as the zero in $(0, 1)$ of (2.19). This should be compared with the polynomials in Fig. 1.

2.3.3. Bounds for the optimal parameters and optimal values. In this section we show that the sequence of optimal parameters a_k^* approaches 0 at least as fast as $\log(k)^2/k^2$. By means of the latter property we can state upper and lower bounds for the optimal values Λ_k .

THEOREM 2.4. *Let Λ_k be the constant defined at (2.16) and let $a_k^* \in (0, 1)$ be such that*

$$\max_{x \in (0,1)} x \left| 1 - \frac{1}{1 - \tau_k^{[a_k^*,1]}(x)^2} \right| = \Lambda_k.$$

If $k \geq 3$, then

$$\frac{\log(k)^2}{9k^2} \leq a_k^* \leq \frac{\log(k)^2}{k^2}, \quad \text{and} \quad \frac{\log(k)}{6k^2} \leq \Lambda_k \leq 1.03 \cdot \frac{\log(k)}{2k^2}.$$

Proof. Let $\varphi(x) := 8k(1 - x^2)^{2k} + x[(1 - x)^{4k} - (1 + x)^{4k}]$ and note that the function φ is negative on the right of its root $\sqrt{a_k^*}$ and positive on its left, i.e., for

$x \in (0, 1)$:

$$\begin{cases} \varphi(x) \leq 0 & \Rightarrow & x^2 \geq a_k^* \\ \varphi(x) \geq 0 & \Rightarrow & x^2 \leq a_k^* \end{cases}.$$

To prove the first claim it is sufficient to show that for $k \geq 3$ we have $\varphi\left(\frac{\log(k)}{k}\right) \leq 0$, and $\varphi\left(\frac{\log(k)}{3k}\right) \geq 0$. By means of some elementary computations we obtain

$$\varphi\left(\frac{\log(k)}{k}\right) \leq 0 \quad \Leftrightarrow \quad \left(\frac{k + \log(k)}{k - \log(k)}\right)^{2k} - \left(\frac{k - \log(k)}{k + \log(k)}\right)^{2k} \geq \frac{8k^2}{\log(k)}.$$

To get the above inequality we observe that

$$\begin{aligned} \left(\frac{k + \log(k)}{k - \log(k)}\right)^{2k} - \left(\frac{k - \log(k)}{k + \log(k)}\right)^{2k} &\geq \left(\frac{k + \log(k)}{k - \log(k)}\right)^{2k} - 1 \\ &= \left[\left(1 + \frac{2 \log(k)}{k - \log(k)}\right)^{\frac{k - \log(k)}{2 \log(k)}} \right]^{\frac{4k \log(k)}{k - \log(k)}} - 1 \\ &\geq 2^{\frac{4k \log(k)}{k - \log(k)}} - 1 \\ &= k^{\frac{4k}{\log(2)(k - \log(k))}} - 1 \\ &\geq k^4 - 1, \end{aligned}$$

and that $k^4 - 1 \geq 8k^2$ —thus greater than $\frac{8k^2}{\log(k)}$ as well—for any $k \geq 3$.

For the lower bound, we have that $\varphi\left(\frac{\log(k)}{3k}\right) \geq 0$ if and only if

$$\left(\frac{3k + \log(k)}{3k - \log(k)}\right)^{2k} - \left(\frac{3k - \log(k)}{3k + \log(k)}\right)^{2k} \leq \frac{24k^2}{\log(k)}.$$

Then, observe that

$$\begin{aligned} \left(\frac{3k + \log(k)}{3k - \log(k)}\right)^{2k} - \left(\frac{3k - \log(k)}{3k + \log(k)}\right)^{2k} &\leq \left(\frac{3k + \log(k)}{3k - \log(k)}\right)^{2k} \\ &\leq \exp\left(\frac{4k \log(k)}{3k - \log(k)}\right) \\ &\leq k^{\frac{12}{9 - \log(3)}}, \end{aligned}$$

and that $k^{\frac{12}{9 - \log(3)}} \leq \frac{24k^2}{\log(k)}$ for any $k \geq 3$.

In view of the argument used to determine a_k^* we see that to get an upper bound for Λ_k it is sufficient to compute an upper bound for $\theta\left(\frac{\log(k)}{k}\right)$ with

$$\theta(x) := \frac{x(1+x)^{2k} + (1-x)^{2k}}{2k(1+x)^{2k} - (1-x)^{2k}}.$$

Once again, some elementary computations yield

$$\theta\left(\frac{\log(k)}{k}\right) = \frac{\log(k)}{2k^2} \cdot \frac{1 + \left(1 - \frac{2 \log(k)}{k + \log(k)}\right)^{2k}}{1 - \left(1 - \frac{2 \log(k)}{k + \log(k)}\right)^{2k}}. \quad \square$$

To get the inequality in the claim it is sufficient to note that the right factor in the above expression is a decreasing function of k , and for $k = 3$ it takes a value of approximately 1.0201 that we can safely bound with 1.03.

Finally, to get a lower bound for Λ_k we compute a lower bound for $\theta\left(\frac{\log(k)}{3k}\right)$:

$$\theta\left(\frac{\log(k)}{3k}\right) = \frac{\log(k)}{6k^2} \cdot \frac{1 + \left(1 - \frac{2\log(k)}{3k + \log(k)}\right)^{2k}}{1 - \left(1 - \frac{2\log(k)}{3k + \log(k)}\right)^{2k}} \geq \frac{\log(k)}{6k^2}.$$

In Figure 4 we show the bounds obtained in Theorem 2.4 for the values of $\{a_k^*\}_k$, and $\{\Lambda_k\}_k$. In Figure 5 we show the computed values of $\{\Lambda_k\}_k$ for the 1st-kind Chebyshev polynomials, compared with the computed values of the bounds for the 4th-kind Chebyshev polynomials and the lower bound for the numerically-approximated optimal 4th-kind Chebyshev polynomials. We observe that for low values of k , i.e., $k \leq 6$, the bound obtained with the optimization of the Chebyshev polynomials of the 1st-kind is lower than that obtained with those of the 4th-kind in (2.10). We also observe that for $k > 1$ the bound is larger than the lower bound corresponding to the optimal 4th-kind Chebyshev polynomials.

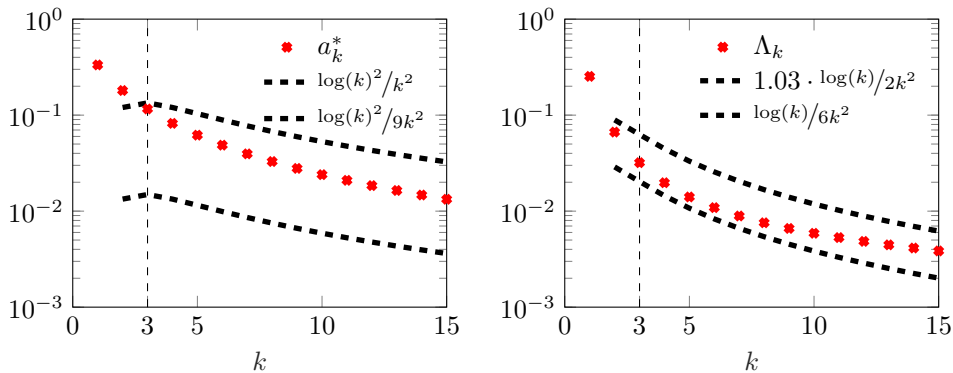


Fig. 4: Bounds and computed quantities for the optimal parameters a_k^* for the 1st-kind Chebyshev polynomials and the smoothing constant Λ_k , $k = 1, \dots, 15$.

3. Implementation details and integration in PSCToolkit. The efficient use of the various levels of memory available in GPU accelerators is crucial for achieving high performance in parallel computing applications; similarly to other devices, NVIDIA GPUs contain various memory levels. The global memory is typically quite large but exhibits a very high latency, of the order of hundreds of cycles, thus necessitating careful programming to hide the cost of its access; the bandwidth depends on the specific card model, and while for high-end devices it can be significantly larger than the bandwidth available on normal CPU memory, it is still much slower than the combined execution rate of the arithmetic units. Shared memory, on the other hand, has a much lower latency and higher bandwidth, and can act as a programmable cache enabling faster data exchange, but only among threads within the same thread block: proper utilization of shared memory can significantly reduce global memory accesses and improve kernel performance. GPUs also have registers allocated per-thread, and they are used for storing private data of individual threads; these are

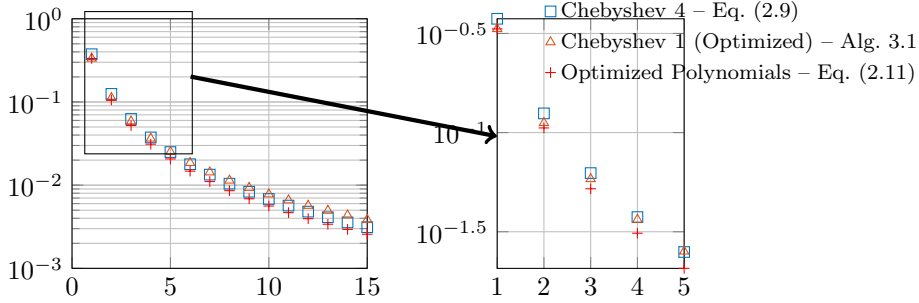


Fig. 5: Comparison of computed bound of the quasi-optimal 1st-kind (2.15) and 4th-kind Chebyshev polynomials (2.9) and the numerically optimized polynomials expressed in terms of the 4th-kind Chebyshev (2.11), for $k = 1, \dots, 15$. The enlargement on the right shows where polynomials of the 1st-kind return a better bound than those of the 4th.

very fast, but their combined size is limited. Balancing the usage of these different memory types by strategically placing data in the most appropriate memory space can drastically enhance the efficiency of GPU kernels. If we transform the recurrences necessary to apply the polynomial smoother based on Chebyshev polynomials of the first type to equation (2.15) into an algorithmic form we obtain the version described in Algorithm 3.1. From this formulation we can observe that the sequence of `axpy`

Algorithm 3.1 Chebyshev acceleration for the polynomial defined in the recurrence relation (2.14) and a fixed-point iteration with matrix M .

```

1: function CHEBYSHEVACCELERATION( $A, \mathbf{b}, \mathbf{x}^{(0)}, M, a, k$ )
2:    $\mathbf{r}^{(0)} \leftarrow \frac{1}{\rho(M^{-1}A)} M^{-1}(\mathbf{b} - A\mathbf{x}^{(0)})$ 
3:    $\sigma_1 \leftarrow \theta/\delta$ 
4:    $\rho_0 \leftarrow 1/\sigma_1$ 
5:    $\mathbf{d}^{(0)} \leftarrow \mathbf{r}^{(0)}/\theta$ 
6:    $\mathbf{x}^{(1)} \leftarrow \mathbf{x}^{(0)} + \mathbf{d}^{(0)}$ 
7:   for  $j = 1, \dots, k - 1$  do
8:      $\mathbf{s}^{(j)} \leftarrow \frac{1}{\rho(M^{-1}A)} M^{-1} A \mathbf{d}^{(j-1)}$ 
9:      $\rho_j \leftarrow (2\sigma_1 - \rho_{j-1})^{-1}$ 
10:     $\mathbf{r}^{(j)} \leftarrow \mathbf{r}^{(j-1)} - \mathbf{s}^{(j)}$ 
11:     $\mathbf{d}^{(j)} \leftarrow \rho_j \rho_{j-1} \mathbf{d}^{(j-1)} + \frac{2\rho_j}{\delta} \mathbf{r}^{(j)}$ 
12:     $\mathbf{x}^{(j+1)} \leftarrow \mathbf{x}^{(j)} + \mathbf{d}^{(j)}$ 
13:   end for
14:   return  $\mathbf{x}^{(k)}$ 
15: end function

```

calls at lines 10, 11 and 12 accesses the same vectors multiple times; it is therefore advisable to minimize the number of accesses to global memory by making explicit use of shared memory, e.g. delaying the store operations of lines 10 and 11. In a more conventional CPU programming context, these optimizations are handled implicitly

by the combined action of the memory hierarchy and cache memory policies, and the compiler optimizations; however in a GPU context it is often necessary to pay explicit attention to such low-level details in the user code. The evolution of programming tools promises to address and alleviate these issues may; however at this time we have chosen to implement an ad-hoc kernel called `psb_upd_xyz(a,b,g,d,x,y,z,desc,info)` to handle the vector updates minimizing the data movements to/from global memory. With this implementation, the cost of applying k steps of the basic ℓ_1 -Jacobi smoother in terms of arithmetic operations and data movement is indeed the same as that of applying the polynomial smoother in Algorithm 3.1 with a polynomial of degree k , and thus we expect a the time per iteration to be comparable. Note that the kernel can be reused for the implementation of the other two polynomial smoothers based on the use of Chebyshev polynomials of the 4th kind, thus unifying all implementation variants, and enabling the user to concentrate on the effect on the number of iterations provided by the better approximation property.

4. Numerical examples. To test the different polynomial smoothers discussed in the previous section we need to complete the construction of the multigrid methods with a coarsening strategy and a coarse solver. We focus on methods available through the `PSCToolkit` framework. This is a software project aimed to make available parallel Krylov solvers and AMG preconditioners efficient on heterogeneous clusters so that we can leverage on high-throughput multi/many-core processors and large numbers of computing nodes for solving linear systems with a very large number of unknowns and prepare our software framework to face the exascale challenge. AMG preconditioners are set by coarsening based on aggregation of unknowns relying on two different approaches, as summarized in the following. More details on the AMG preconditioners included in `PSCToolkit` we refer the reader to [8, 9].

VBM the classical smoothed aggregation strategy by Vaněk, Mandel, and Brezina [23], that is adapted to the distributed setting in a *decoupled* way, i.e., for which the aggregates are determined only on the local part of the matrix of that level;

Compatible Matching the aggregation strategy based on graph weighted matching and compatible relaxation [10, 8], that is instead a parallel *coupled* strategy which relies on the computation of an approximate graph weighted matching of the whole adjacency matrix. For this choice the maximum size of the requested aggregates can be selected in input as a power of 2, i.e., it corresponds on the number of the matching application we perform at each level. The prolongator obtained by this construction can be used as tentative prolongator for a classic smoothing procedure as in [23], i.e., if we call \hat{P}_l the tentative prolongator obtained via the matching strategy at level l , the one we actually use is

$$P_l = (I - \omega D_l^{-1} A_l) \hat{P}_l,$$

for D_l the diagonal of A_l , and $\omega = 4/3\lambda_{\max}$ for λ_{\max} an estimate of the largest eigenvalue of $D_l^{-1} A_l$.

Both the types of the AMG hierarchies can be employed as standard V -Cycle (2.1) in the application phase as preconditioner for a Krylov solver. For the experiments discussed in this paper, at the coarsest level we applied a fixed (sufficiently large) number of iteration of the highly parallel ℓ_1 -Jacobi method. Table 1 succinctly summarizes the different building blocks we use.

To test the proposed strategy we consider linear systems (1.1) arising from usual benchmarks, as described in the following.

Table 1: The table contains the building blocks from `PSCToolkit` we use to build the preconditioners we consider.

| Pre/Post-smoother | Aggregation | Cycle | Coarse |
|---|---------------------|---------|------------------|
| ℓ_1 -Jacobi | VBM | V-Cycle | ℓ_1 -Jacobi |
| Chebyshev 4 th -kind | Compatible Matching | | |
| Optimized Chebyshev 4 th -kind | | | |
| Optimized Chebyshev 1 st -kind | | | |

Poisson 3D: the matrix A comes from the usual 7-points discretization of the Poisson equation on the unit cube, when Dirichlet boundary conditions are applied and right-hand side is set equal to the unit vector.

Anisotropy 2D: the matrix A comes from an anisotropic 2D thermal problem with Q1-finite element methods on the domain $[-1, 1]^2$, and the material conductivity given by the tensor

$$\mathcal{K}_\epsilon = \begin{bmatrix} 1 & 0 \\ 0 & \epsilon \end{bmatrix}$$

rotated by an angle θ around the origin, Dirichlet boundary conditions fixed on the $y = -1$ face of the square, and right-hand side given by the discretization of

$$f(x, y) = \exp(-100(x^2 + y^2)).$$

For all cases the iterative method of choice is a variant of the Conjugate Gradient (CG), requiring only one global synchronization for scalar products [21], and is set to achieve a relative tolerance on the error of $tol = 10^{-7}$ within a maximum number of iteration $it_{\max} = 1000$. The experiments were performed on the Leonardo Italian supercomputer, ranked 7th in the June 2024 Top500 list (BullSequana XH2000, Xeon Platinum 8358 32C 2.6GHz, NVIDIA A100 SXM4 64 GB, Quad-rail NVIDIA HDR100 Infiniband). The code, execution scripts and the pointers to the `PSCToolkit` packages versions used are available on the GitHub repository `Cirdans-Home/polynomialsmoothers`.

4.1. Weak scalability experiments. We conduct weak scalability experiments using the two preconditioners described at the beginning of Section 4. More specifically, we maintain a fixed number of degrees of freedom per computational unit (GPU) while linearly increasing both the problem size and the number of GPUs involved, ranging from 64 to 1024 GPUs (i.e., from 16 to 256 computing nodes). In these experiments, the key metrics of interest are the solution time, which indicates the method’s efficiency for the user and its utility within more complex simulations; the number of iterations, which illustrates the theoretical properties of the considered polynomial acceleration; and the time per iteration, which measures the efficiency of the method’s implementation.

4.1.1. Poisson 3D. For linear systems of the Poisson 3D test case, we present results for the multigrid preconditioner based on compatible matching aggregation because it always produces the smallest number of iterations. These results are complemented by additional data in the supplementary materials, which include higher degree polynomial smoothers (Section 1.1.1) and the preconditioner based on VBM aggregation (Section 1.1.2).

Compatible Matching. We first look at the solution time with different smoothers as the number of GPUs increases; As expected, all the polynomial accelerators reduces

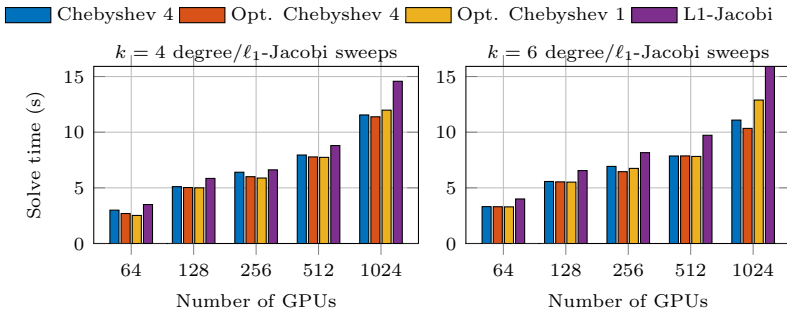


Fig. 6: Solve time (s). Time to solution (s) for the Poisson 3D test case employing the multigrid scheme based on the compatible matching aggregation in conjunction with the different polynomial accelerators and the baseline ℓ_1 -Jacobi for comparison.

the solve time with respect to the baseline ℓ_1 -Jacobi; the reduction is more significant as the problem size increases and as polynomial degree (number of baseline iterations) increases. For a low degree ($k = 4$), the quasi-optimal 1st-kind Chebyshev polynomial is better or comparable with the optimized 4th-kind ones. Their application produces the best solution times for all the number of GPUs but the largest one, where we observe the best solve time for the optimized 4th-kind polynomials when $k = 6$. This confirms that having a polynomial smoother that performs well for low polynomial degrees can be extremely effective. In other words, the initial transient behavior of the estimate turns out to be more relevant than the asymptotic behavior in the degree. It is worth to note that using polynomial accelerations results in a solve time reduction ranging from $\approx 18\%$ to $\approx 35\%$ for the largest problem size. This gain in the solve times comes from the better convergence properties of the polynomial accelerators and from the efficiency of their GPU implementation, as shown in Fig. 7 and Fig. 8, respectively. Indeed, if we investigate the number of iterations, we observe that, in a good agreement with the bound behaviour in Fig. 5, the quasi-optimal 1st-kind Chebyshev polynomial and the optimized 4th-kind ones return the same number of iterations for $k = 4$, while in the case of $k = 6$, the optimized 4th-kind polynomials reduces the number of iterations more than the other approaches when solving the largest size problem. In particular, we observe that increasing polynomial degree from $k = 4$ to $k = 6$ reduces the number of iterations from 18 to 14 in the case of the optimized 4th-kind while we go from 18 to 15 for the quasi-optimal 1st-kind. On the contrary the baseline is able to reduce the iterations only from 21 to 20. The times per iteration of the different polynomial accelerators remain fully comparable to those of the ℓ_1 -Jacobi method, showing that the advantage in the approximation properties of the polynomial smoother does not increase the computational cost of the entire solution procedure.

4.1.2. Anisotropy 2D. We examine the problem based on the 2D diffusion operator with anisotropy, specifically for an anisotropy angle of $\theta = \pi/6$ and a coefficient value of $\epsilon = 100$. In this case, the best results are obtained when the multigrid preconditioner setup is based on the VBM classical smoothed aggregation. These experiments are supplemented by additional results in the supplementary materials,

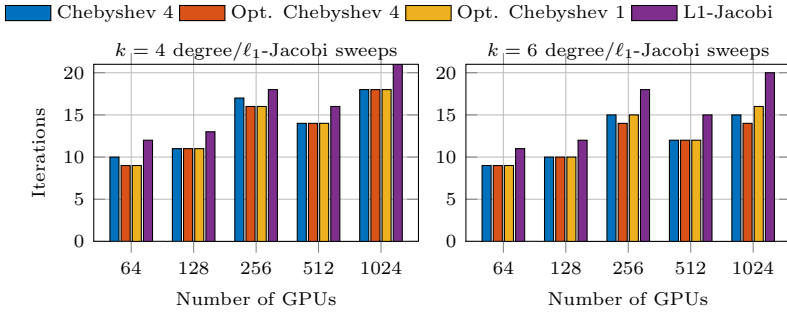


Fig. 7: Iteration count. Total number of CG iterations for the Poisson 3D test case employing the multigrid scheme based on the compatible matching aggregation in conjunction with the different polynomial accelerators and the baseline ℓ_1 -Jacobi for comparison.

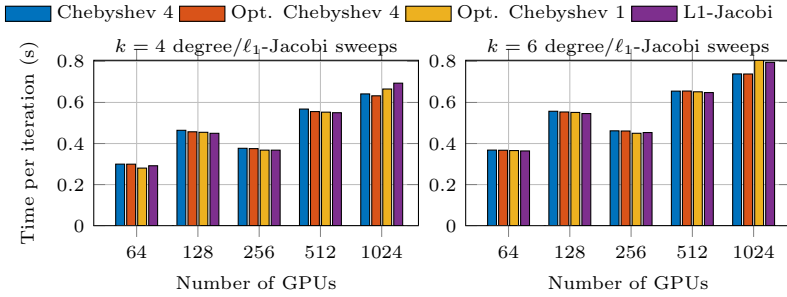


Fig. 8: Time per iteration. Time per iteration for the Poisson 3D test case employing the multigrid scheme based on the compatible matching aggregation in conjunction with the different polynomial accelerators and the baseline ℓ_1 -Jacobi for comparison.

which include higher polynomial degrees (Section 1.2.1) and multigrid with aggregation based on matching (Section 1.2.2).

VBM. As in the previous section, in Fig. 9 we report the time needed to reach the solution of the linear system by keeping the multigrid preconditioner hierarchy fixed and changing the smoother and the polynomial smoother degree (or number of smoothing iterations for the ℓ_1 -Jacobi). As for the previous test case, using the polynomial accelerations generally reduces the solve times although the percentage of the reduction is smaller than in the results discussed in the previous section. This demonstrates a smaller impact of the quality of the smoother in this type of preconditioner based on classical smoothed aggregation, as also shown in the results on the Poisson 3D test case reported in the supplementary materials. The time needed to reach a solution is always lower for the preconditioner using the lightest smoother, i.e., the one with the smallest degree of the polynomial acceleration or, equivalently, the smallest number of matrix-vector products. It is generally obtained when the optimized 4th-kind polynomials are applied when the number of GPUs increases. Indeed, if we turn our attention to Fig. 10, the version based on the optimized 4th-kind polynomials produces the smallest number of iterations for both the polynomial degrees, while, as

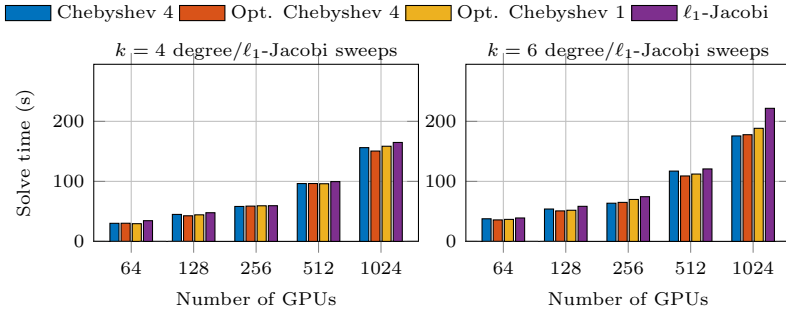


Fig. 9: Solve time (s). Time to solution (s) for the Anisotropy 2D test case ($\varepsilon = 100, \theta = \pi/6$) employing the multigrid scheme based on the VBM aggregation in conjunction with the different polynomial accelerators and the baseline ℓ_1 -Jacobi for comparison.

expected, the quasi-optimal 1st-kind ones are comparable to the optimized 4th-kind polynomials when the lowest degree is used. Applying polynomials accelerators with a larger degree rewards in terms of number of iteration to obtain the given accuracy, but does not pay in terms of total solve times, i.e., the reduction in the number of iterations is not sufficient to balance the cost of the increasing application cost per iteration as shown in Fig. 11. This cost is generally consistent with that of applying a corresponding number of iterations of the ℓ_1 -Jacobi method. That is, we can confirm that from a node-level efficiency perspective and thanks to the careful implementation of shared memory accesses and GPU threads, the use of polynomial smoothers with better approximation capability is achieved practically at a cost that falls within the machine’s oscillations.

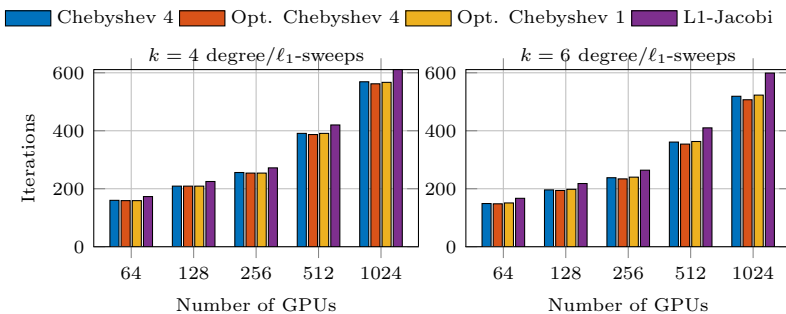


Fig. 10: Iteration count. Total number of CG iterations for the Anisotropy 2D test case ($\varepsilon = 100, \theta = \pi/6$) employing the multigrid scheme based on the VBM aggregation in conjunction with the different polynomial accelerators and the baseline ℓ_1 -Jacobi for comparison.

5. Conclusion. In this paper, we have demonstrated the benefits of using polynomial smoothers based on Chebyshev polynomials to accelerate the basic ℓ_1 -Jacobi smoother, particularly in the context of large-scale GPU deployment. We have also

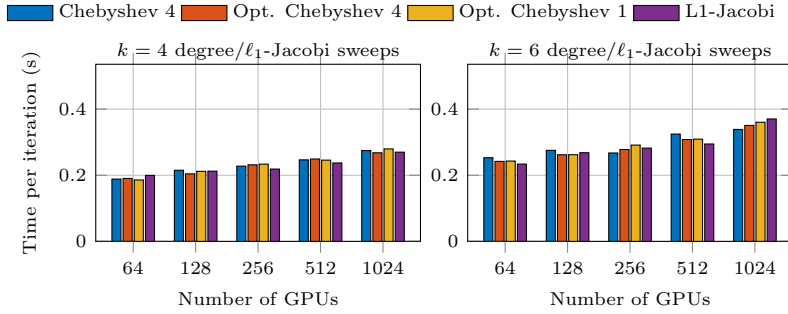


Fig. 11: Time per iteration. Time per iteration for the Anisotropy 2D test case ($\varepsilon = 100, \theta = \pi/6$) employing the multigrid scheme based on the VBM aggregation in conjunction with the different polynomial accelerators and the baseline ℓ_1 -Jacobi for comparison.

shown that optimizing the convergence bound using 1st-kind Chebyshev polynomials achieves superior convergence properties for low-degree polynomial accelerators compared to 4th-kind Chebyshev polynomials. As expected, the impact of using polynomial accelerators also depends on the interplay with the type of coarsening procedures and then of the quality of the AMG hierarchies. From an implementation perspective, we illustrated how efficient memory management on GPUs allows the application cost of a k -degree polynomial accelerator to match that of k applications of the basic smoother, despite the increased number of `axpy` operations.

To further extend the applicability of our methods, we plan to investigate solving minimax problems in the complex plane, targeting non-symmetric linear systems that arise from discretizing sectorial differential operators. Additionally, we anticipate that using inter-vector operations in our kernels will enable us to leverage technologies like OpenACC, achieving similar performance with lower maintenance costs. We also aim to make our library hardware-agnostic, ensuring compatibility beyond NVIDIA GPUs. These future endeavors will enhance the robustness and versatility of our approach in various high-performance computing scenarios.

Appendix A. Proof of Lemma 2.2, and Lemma 2.3. Here we report the proofs of the two lemmas concerning the minimax approximation with Chebyshev polynomials of the 1st kind.

Proof of Lemma 2.2. Observe that we can write $f(x) = f_1(x) \cdot f_2(x)$ where

$$f_1(x) := \frac{x\tau_k^{[a,1]}(x)}{1 - \tau_k^{[a,1]}(x)}, \quad f_2(x) := \frac{\tau_k^{[a,1]}(x)}{1 + \tau_k^{[a,1]}(x)},$$

and f_1, f_2 are both positive functions on $(0, a]$. Moreover, $f_2(x)^{-1} = 1 + \frac{1}{\tau_k^{[a,1]}(x)}$ is monotonically increasing on $(0, a]$ and this implies that f_2 is monotonically decreasing on $(0, a]$. We will show that also f_1 is monotonically decreasing and this will give us the claim as the product of non negative decreasing functions is also decreasing.

Let us indicate with $p(x) := \tau_k(\frac{1+a-2x}{1-a})$ and $c_k := \tau_k(\frac{1+a}{1-a})$, so that $\tau_k^{[a,1]}(x) =$

$p(x)/c_k$. Studying the negativity of the derivative of f_1 yields

$$\begin{aligned}
\frac{df_1}{dx}(x) &= \frac{\tau_k^{[a,1]}(x) \left(1 - \tau_k^{[a,1]}(x)\right) + x(\tau_k^{[a,1]})'(x)}{\left(1 - \tau_k^{[a,1]}(x)\right)^2} < 0 && \text{for } x \in (0, a] \\
&\Leftrightarrow \tau_k^{[a,1]}(x) \left(1 - \tau_k^{[a,1]}(x)\right) + x(\tau_k^{[a,1]})'(x) < 0 && \text{for } x \in (0, a] \\
&\Leftrightarrow p(x) \left(1 - \frac{p(x)^2}{c_k}\right) + xp'(x) < 0 && \text{for } x \in (0, a] \\
&\Leftrightarrow 1 - \frac{p(x)}{c_k} + x \frac{p'(x)}{p(x)} < 0 && \text{for } x \in (0, a],
\end{aligned}$$

where we have used that $c_k > 0$ and that $p(x) > 0$ on $(0, a]$.

We now show that the function $-\frac{p(x)}{c_k} + x \frac{p'(x)}{p(x)}$ is monotonically decreasing and this implies the claim since $1 - \frac{p(x)}{c_k} + x \frac{p'(x)}{p(x)}$ takes the value 0 at $x = 0$. Taking the derivative yields

$$\begin{aligned}
\frac{d}{dx} \left(-\frac{p(x)}{c_k} + x \frac{p'(x)}{p(x)} \right) &= \frac{x(p''(x)p(x) - p'(x)^2)}{p(x)^2} < 0 && \text{for } x \in (0, a] \\
&\Leftrightarrow p''(x)p(x) - p'(x)^2 < 0 && \text{for } x \in (0, a] \\
&\Leftrightarrow \frac{p''(x)}{p'(x)} - \frac{p'(x)}{p(x)} > 0 && \text{for } x \in (0, a] \\
&\Leftrightarrow \frac{d}{dx} \left(\log \left(-\frac{p'(x)}{p(x)} \right) \right) > 0 && \text{for } x \in (0, a] \\
&\Leftrightarrow \log \left(-\frac{p'(x)}{p(x)} \right) \text{ is increasing} && \text{for } x \in (0, a],
\end{aligned}$$

where we have used that $p(x) > 0$ and $p'(x) < 0$ on $(0, a]$. Since the logarithm is increasing, it is sufficient to show that $-\frac{p'(x)}{p(x)}$ is also increasing. Note that $\frac{p'(x)}{p(x)} = \frac{d}{dx}(\log(p(x)))$ and that

$$\log(p(x)) = \log \left(c_k \prod_{j=1}^k (x_j - x) \right) = \log(c_k) + \sum_{j=1}^k \log(x_j - x),$$

where the quantities $x_j \in (a, 1)$ are the roots of $p(x)$, for $j = 1, \dots, k$. In particular, $\log(p(x))$ is a concave function (being the sum of concave functions) and this yields

$$0 > -\frac{d^2}{dx^2}(\log(p(x))) = \frac{d}{dx} \left(-\frac{p'(x)}{p(x)} \right),$$

that implies the claim. \square

Proof of Lemma 2.3. Let us define the polynomials $p(x) = \sum_{j=0}^k \binom{2k}{2j} x^j$ with roots $\alpha_1, \dots, \alpha_k$, and $q(x) = \sum_{j=0}^{k-1} \binom{2k}{2j+1} x^j$ with roots $\delta_1, \dots, \delta_{k-1}$. We begin by showing that the roots of the $p(x)$ and $q(x)$ are all negative real and verify the interlacing property:

$$(A.1) \quad 0 > \alpha_1 > \delta_1 > \alpha_2 > \delta_2 > \dots > \alpha_{k-1} > \delta_{k-1} > \alpha_k.$$

Note that if γ is a root of $p(x^2)$ then γ^2 is equal to α_i for a certain $i = 1, \dots, k$. Moreover, we have

$$p(x^2) = \sum_{j=0}^k \binom{2k}{2j} x^{2j} = \frac{1}{2}[(1+x)^{2k} + (1-x)^{2k}],$$

so that $p(x^2) = 0$ if and only if $|1+x| = |1-x|$. The latter implies that all the roots are of the form $x = \mathbf{i}b$ with $b \in \mathbb{R}$. Then,

$$\begin{aligned} p((\mathbf{i}b)^2) &= \operatorname{Re}((1 + \mathbf{i}b)^{2k}) = 0 \\ \Leftrightarrow \operatorname{Arg}(1 + \mathbf{i}b) &= \frac{(2j+1)\pi}{4k}, \quad j = 0, \dots, 2k-1, \\ \Leftrightarrow \arctan(b) &= \frac{(2j+1)\pi}{4k}, \quad j = 0, \dots, 2k-1, \\ \Rightarrow \text{the roots of } p(x) &\text{ are } \alpha_j = -\tan\left(\frac{(2j+1)\pi}{4k}\right)^2, \quad j = 0, \dots, k-1. \end{aligned}$$

Similarly, we have

$$xq(x^2) = \sum_{j=0}^{k-1} \binom{2k}{2j+1} x^{2j+1} = \frac{1}{2}[(1+x)^{2k} - (1-x)^{2k}],$$

and if γ is a nonzero root of $xq(x^2)$ then $\gamma^2 = \delta_j$ for a certain $j = 1, \dots, k-1$. For the same reason of $p(x^2)$, $xq(x^2)$ has only purely imaginary roots of the form $x = \mathbf{i}b$ and

$$\begin{aligned} (\mathbf{i}b) \cdot q((\mathbf{i}b)^2) &= \operatorname{Im}((1 + \mathbf{i}b)^{2k}) = 0 \\ \Leftrightarrow \operatorname{Arg}(1 + \mathbf{i}b) &= \frac{j\pi}{2k}, \quad j = 0, \dots, 2k-1, \\ \Leftrightarrow \arctan(b) &= \frac{j\pi}{2k}, \quad j = 0, \dots, 2k-1, \\ \Rightarrow \text{the roots of } q(x) &\text{ are } \delta_j = -\tan\left(\frac{j\pi}{2k}\right)^2, \quad j = 1, \dots, k-1. \end{aligned}$$

We remark that the values α_j and δ_j verify (A.1).

To conclude, we look at the first derivative of $2k \cdot g(x) = \frac{p(x)}{q(x)}$ over $(0, 1)$:

$$\begin{aligned} 2kg'(x) &= \frac{p'(x)q(x) - p(x)q'(x)}{q(x)^2} > 0 \quad \text{for } x \in (0, 1) \\ \Leftrightarrow \frac{p'(x)}{p(x)} - \frac{q'(x)}{q(x)} &> 0 \quad \text{for } x \in (0, 1) \\ \Leftrightarrow \frac{d}{dx} \left(\log \left(\frac{p(x)}{q(x)} \right) \right) &> 0 \quad \text{for } x \in (0, 1) \\ \Leftrightarrow \sum_{j=1}^{k-1} \frac{d}{dx} \left(\log \left(\frac{x - \alpha_j}{x - \delta_j} \right) \right) + \frac{d}{dx} (\log(x - \alpha_k)) &> 0 \quad \text{for } x \in (0, 1) \\ \Leftrightarrow \sum_{j=1}^{k-1} \frac{\alpha_j - \delta_j}{(x - \alpha_j)(x - \delta_j)} + \frac{1}{x - \alpha_k} &> 0 \quad \text{for } x \in (0, 1). \end{aligned}$$

The latter relation is implied by (A.1), and this gives the claim. \square

REFERENCES

- [1] M. ADAMS, M. BREZINA, J. HU, AND R. TUMINARO, *Parallel multigrid smoothing: polynomial versus Gauss-Seidel*, J. Comput. Phys., 188 (2003), pp. 593–610, [https://doi.org/10.1016/S0021-9991\(03\)00194-3](https://doi.org/10.1016/S0021-9991(03)00194-3).
- [2] H. ANZT, E. BOMAN, R. FALGOUT, AND ET AL., *Preparing sparse solvers for exascale computing*, Philos. Trans. Roy. Soc. A, 378 (2020), pp. 20190053, 17, <https://doi.org/10.1098/rsta.2019.0053>.
- [3] A. H. BAKER, R. D. FALGOUT, T. V. KOLEV, AND U. M. YANG, *Multigrid smoothers for ultraparallel computing*, SIAM J. Sci. Comput., 33 (2011), pp. 2864–2887, <https://doi.org/10.1137/100798806>.
- [4] F. BASSI, A. GHIDONI, AND S. REBAY, *Optimal Runge-Kutta smoothers for the p-multigrid discontinuous Galerkin solution of the 1D Euler equations*, J. Comput. Phys., 230 (2011), pp. 4153–4175, <https://doi.org/10.1016/j.jcp.2010.04.030>.
- [5] D. BERTACCINI, M. DONATELLI, F. DURASTANTE, AND S. SERRA-CAPIZZANO, *Optimizing a multigrid Runge-Kutta smoother for variable-coefficient convection-diffusion equations*, Linear Algebra Appl., 533 (2017), pp. 507–535, <https://doi.org/10.1016/j.laa.2017.07.036>.
- [6] P. BIRKEN, *Optimizing Runge-Kutta smoothers for unsteady flow problems*, Electron. Trans. Numer. Anal., 39 (2012), pp. 298–312.
- [7] O. BRÖKER, M. J. GROTE, C. MAYER, AND A. REUSKEN, *Robust parallel smoothing for multigrid via sparse approximate inverses*, SIAM J. Sci. Comput., 23 (2001), pp. 1396–1417, <https://doi.org/10.1137/S1064827500380623>.
- [8] P. D’AMBRA, F. DURASTANTE, AND S. FILIPPONE, *AMG preconditioners for linear solvers towards extreme scale*, SIAM J. Sci. Comput., 43 (2021), pp. S679–S703, <https://doi.org/10.1137/20M134914X>.
- [9] P. D’AMBRA, F. DURASTANTE, AND S. FILIPPONE, *Parallel sparse computation toolkit*, Software Impacts, 15 (2023), <https://doi.org/10.1016/j.simpa.2022.100463>.
- [10] P. D’AMBRA, S. FILIPPONE, AND P. S. VASSILEVSKI, *BootCMatch: a software package for bootstrap AMG based on graph weighted matching*, ACM Trans. Math. Software, 44 (2018), pp. Art. 39, 25, <https://doi.org/10.1145/3190647>.
- [11] G. E. FORSYTHE, M. A. MALCOLM, AND C. B. MOLER, *Computer methods for mathematical computations*, Prentice-Hall Series in Automatic Computation, Prentice-Hall, Inc., Englewood Cliffs, NJ, 1977.
- [12] P. GHYSELS, P. KLOSIEWICZ, AND W. VANROOSE, *Improving the arithmetic intensity of multigrid with the help of polynomial smoothers*, Numer. Linear Algebra Appl., 19 (2012), pp. 253–267, <https://doi.org/10.1002/nla.1808>, <https://doi.org/10.1002/nla.1808>.
- [13] G. H. GOLUB AND R. S. VARGA, *Chebyshev semi-iterative methods, successive over-relaxation iterative methods, and second order Richardson iterative methods. II*, Numer. Math., 3 (1961), pp. 157–168, <https://doi.org/10.1007/BF01386014>.
- [14] W. HACKBUSCH, *Multigrid convergence theory*, in Multigrid methods (Cologne, 1981), vol. 960 of Lecture Notes in Math., Springer, Berlin-New York, 1982, pp. 177–219.
- [15] R. HUANG, R. LI, AND Y. XI, *Learning optimal multigrid smoothers via neural networks*, SIAM J. Sci. Comput., 45 (2023), pp. S199–S225, <https://doi.org/10.1137/21M1430030>.
- [16] J. KRAUS, P. VASSILEVSKI, AND L. ZIKATANOV, *Polynomial of best uniform approximation to and smoothing in two-level methods*, Computational Methods in Applied Mathematics, 12 (2012), pp. 448–468, <https://doi.org/doi:10.2478/cmam-2012-0026>, <https://doi.org/10.2478/cmam-2012-0026>.
- [17] S. LANGER, *Agglomeration multigrid methods with implicit Runge-Kutta smoothers applied to aerodynamic simulations on unstructured grids*, J. Comput. Phys., 277 (2014), pp. 72–100, <https://doi.org/10.1016/j.jcp.2014.07.050>.
- [18] J. LOTTES, *Optimal polynomial smoothers for multigrid V-cycles*, Numer. Lin. Alg. with Appl., 30 (2023), p. e2518, <https://doi.org/10.1002/nla.2518>.
- [19] J. C. MASON AND D. C. HANDSCOMB, *Chebyshev polynomials*, Chapman & Hall/CRC, Boca Raton, FL, 2003.
- [20] S. F. MCCORMICK, *Multigrid methods for variational problems: general theory for the V-cycle*, SIAM J. Numer. Anal., 22 (1985), pp. 634–643, <https://doi.org/10.1137/0722039>.
- [21] Y. NOTAY AND A. NAPOV, *A massively parallel solver for discrete Poisson-like problems*, Journal of Computational Physics, 281 (2015), pp. 237–250, <https://doi.org/https://doi.org/10.1016/j.jcp.2014.10.043>, <https://www.sciencedirect.com/science/article/pii/S0021999114007256>.
- [22] P. VANĚK AND M. BREZINA, *Nearly optimal convergence result for multigrid with aggressive coarsening and polynomial smoothing*, Appl. Math., 58 (2013), pp. 369–388, <https://doi.org/https://doi.org/10.1007/s11464-013-0369-8>.

- org/10.1007/s10492-013-0018-2.
- [23] P. VANĚK, J. MANDEL, AND M. BREZINA, *Algebraic multigrid by smoothed aggregation for second and fourth order elliptic problems*, vol. 56, 1996, pp. 179–196, <https://doi.org/10.1007/BF02238511>. International GAMM-Workshop on Multi-level Methods (Meisdorf, 1994).
 - [24] P. S. VASSILEVSKI, *Multilevel block factorization preconditioners*, Springer, New York, 2008. Matrix-based analysis and algorithms for solving finite element equations.
 - [25] J. XU AND L. ZIKATANOV, *Algebraic multigrid methods*, *Acta Numer.*, 26 (2017), pp. 591–721, <https://doi.org/10.1017/S0962492917000083>.

SUPPLEMENTARY MATERIALS: OPTIMAL POLYNOMIAL SMOOTHERS FOR PARALLEL AMG

These supplementary materials contain fine details regarding the numerical experiments on the test cases (Section 1), and the instruction to use the polynomial smoothers inside the `PSCToolkit` library (Section 2).

Appendix 1. Additional details on the numerical experiments in Section 4. The experimental setting is exactly the same, both from the computing point of view and from the point of view of the software requirements. The sections are mirrors of those contained in the paper.

1.1. Poisson 3D. The following two sections contain additional information regarding the Poisson 3D problem. They extend the results contained in Section 4.1.1 adding to the considerations the effect of the smoothers for a higher degree of the polynomial and the use of the compatible matching aggregation.

1.1.1. Compatible Matching. In Fig. 6 we reported the time needed to reach the solution of the linear system by keeping the multigrid preconditioner hierarchy fixed and changing the smoother and between the different types of polynomial acceleration and with respect to the degree–number of vector matrix products used per iteration; we extend the results in Fig. 12 by considering polynomial of higher degree while plotting all the figures on the same scale. The behavior of the solution times is analogous to that observed for lower degrees in the paper. There is an increase in the total solution time with the increase in the degree of the polynomial used as smoother, however, it is worth to note that the increase ratio observed for the polynomial smoothers is smaller than the increase ratio for the baseline ℓ_1 -Jacobi, especially for increasing problem size and number of GPUs. This confirms the better scalability potential of the polynomial accelerations, in the face of the expected reduction in the number of iterations as k increases shown in Fig. 13. However, the improvement in the number of iterations is not sufficient to amortize the cost of the additional sparse matrix-vector products needed to apply the higher degree polynomial. Hence the error reduction effect due to the smoother is again more important with respect to a low degree polynomial than with respect to a higher degree polynomial. To conclude this set of experiments we can look again at the implementation scalability properties of the method by focusing on the iteration time of the different polynomial smoothers in Fig. 14. Again the iteration time of the different methods is completely comparable with that of the reference method, the proportional growth with respect to the degree k of the polynomial is consistent with the increase in the number of sparse matrix-vector products.

1.1.2. VBM. This set of experiments extends those in Section 4.1.1 of the paper. In Fig. 15 we report the solution times for the different smoothers using in each case the VBM aggregation procedure. What we observe is that again as the number of iterations of the smoother increases, i.e., the degree of the polynomial, the performance in total solution time worsens and the best ones are obtained for the lowest degree. This is even in the face of the reduction in the total number of iterations observed in Fig. 16. The decrease in the number of iterations in the face of the increase in cost in terms of sparse matrix-vector products is not sufficient to lower the total solution time. On the other hand, the algorithmic scalability of the method remains consistent with what has been seen in other cases. The picture in Fig. 17 shows how the cost per

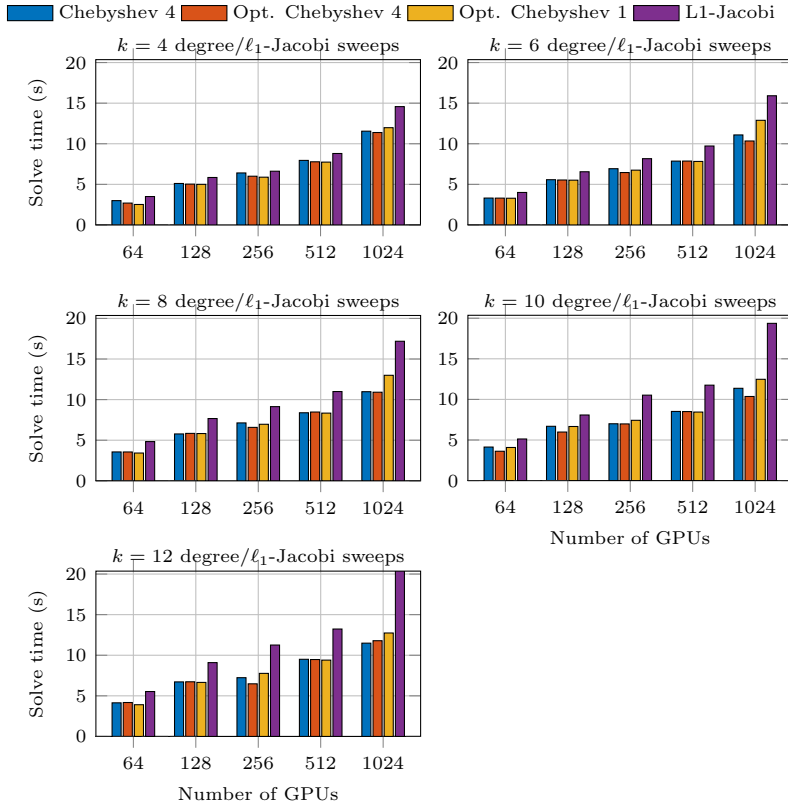


Fig. 12: Solve time (s). Time to solution (s) for the Poisson 3D test case employing the multigrid scheme based on the compatible matching aggregation in conjunction with the different polynomial accelerators and the baseline ℓ_1 -Jacobi for comparison.

iteration remains comparable to that of the ℓ_1 -Jacobi method as the number of GPUs increases. While the cost increases proportionally to the degree of the polynomial, i.e. the number of sparse matrix-vector products used. We finally observe that the time per iteration for the VBM aggregation is smaller than those for the compatible matching coarsening, therefore, although the number of iteration for compatible matching is generally smaller, the solve time obtained with the VBM scheme are smaller due to the smaller operator complexity of the built matrix hierarchies.

1.2. Anisotropy 2D. The following two sections contain additional information regarding the 2D anisotropic problem with angle $\theta = \pi/6$ and $\epsilon = 100$. They extend the results contained in Section 4.1.2 adding to the considerations the effect of the smoothers for a higher degree of the polynomial and the use of matching-based aggregation.

1.2.1. VBM. In Fig. 18 we report the time needed to reach the solution of the linear system by keeping the multigrid preconditioner hierarchy fixed and changing the smoother and between the different types of polynomial acceleration and with respect to the degree–number of sparse matrix-vector products used per iteration; we extend the results in Fig. 9 by considering polynomial of higher degree while plotting

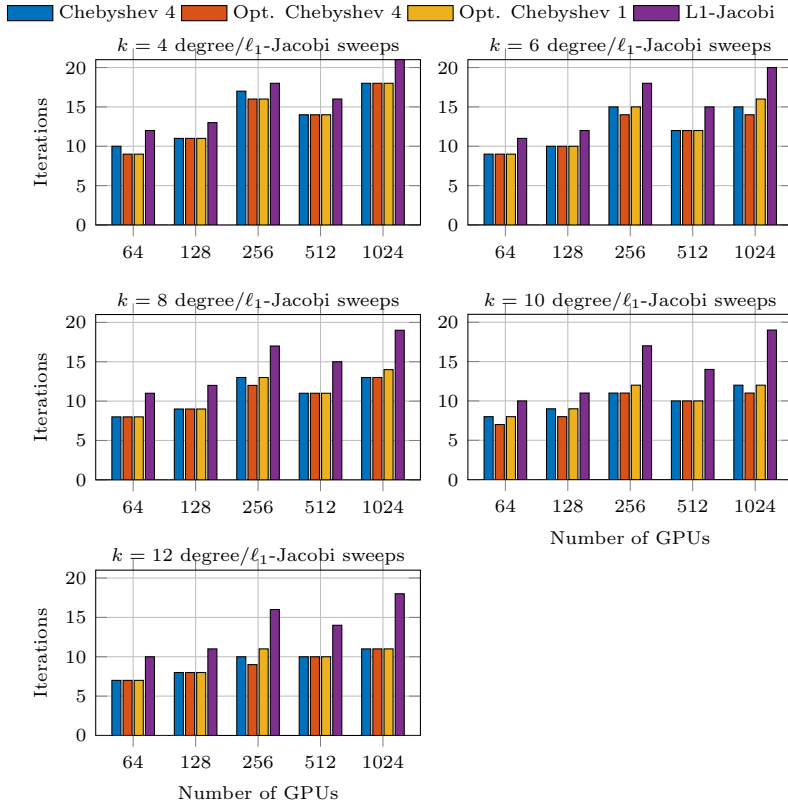


Fig. 13: Iteration count. Total number of FCG iterations for the Poisson 3D test case employing the multigrid scheme based on the compatible matching aggregation in conjunction with the different polynomial accelerators and the baseline ℓ_1 -Jacobi for comparison.

all the figures on the same scale. We observe that the best solution time is obtained for the smoother of lower degree, even if the number of iterations to convergence is decreased with increasing k , as depicted in Fig. 19. The decrease is not sufficient to compensate for the increase in application cost, i.e., the increase in the number of sparse matrix-vector products.

Finally we focus on the scalability of implementing different polynomial smoothers on the GPU, looking at the time per iteration in Fig. 20. As the degree of the polynomial increases, the implementation scalability properties of the method are confirmed. The specific observation to be made is that the time per iteration always remains perfectly comparable with that of the basic smoother which is ℓ_1 -Jacobi and that this grows in the expected manner as the degree k of the polynomial representing the smoother increases. In particular, this shows that our GPU implementation of the different methods behaves consistently with the degree of the polynomial.

1.2.2. Compatible Matching. In the paper, we only report the results for the VBM aggregation-based preconditioner, which achieves the best results on this problem. To complete the overview, we also consider here the solution employing

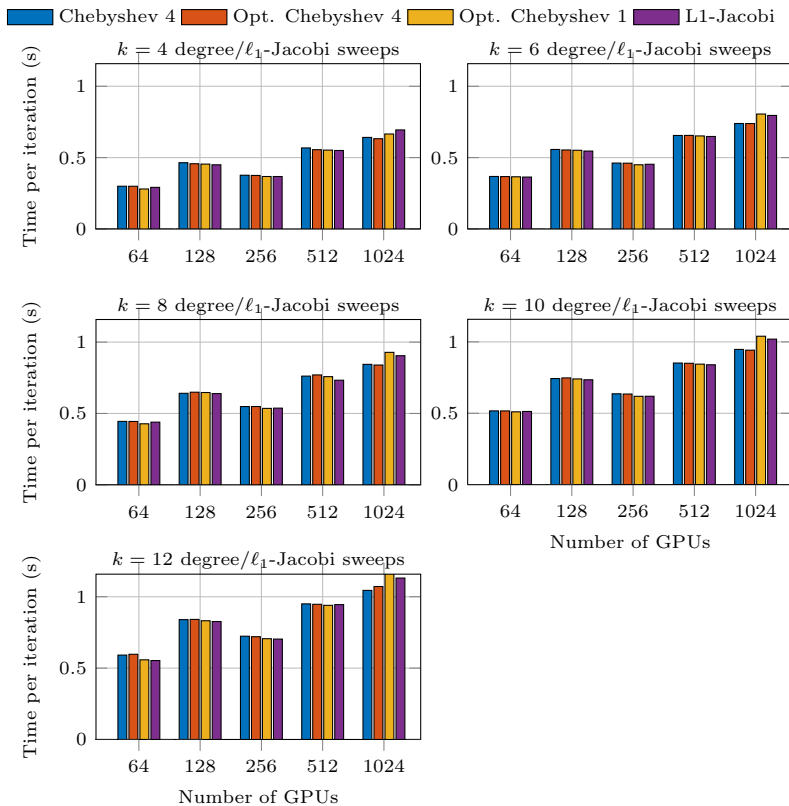


Fig. 14: Time per iteration. Time per iteration for the Poisson 3D test case employing the multigrid scheme based on the compatible matching aggregation in conjunction with the different polynomial accelerators and the baseline ℓ_1 -Jacobi for comparison.

the multigrid preconditioners with aggregation based on the compatible matching strategy while limiting ourselves, due to the limits in core-hours granted, to scaling results up to 512 GPUs. However, this is enough to describe the behavior of the algorithm. As for all the other cases, we start from Fig. 21 where we report the solve time, and we observe that for low values of the degree we obtain both the best results and that the best result is the one with the quasi-optimal Chebyshev polynomials of 1st degree. This confirms the larger impact of the optimized smoothers for this type of coarsening scheme. If we turn now to the iteration count reported in Fig. 22 we observe again a behavior comparable to that analyzed in the case of the VBM aggregation, albeit with a higher overall number of iterations. The behavior with respect to the implementation scalability of the smoothers remains unchanged with respect to the case with the VBM aggregation strategy as shown in Fig. 23.

Appendix 2. Code snippets. In this section we report the instructions needed to configure and setup the preconditioners used in the numerical experiments, together with the calls needed for the assembly phase on the GPU accelerator. To allow the possibility of a code in which the chosen matrix storage format is changed at runtime, either to accommodate different algorithmic needs or to be able to execute

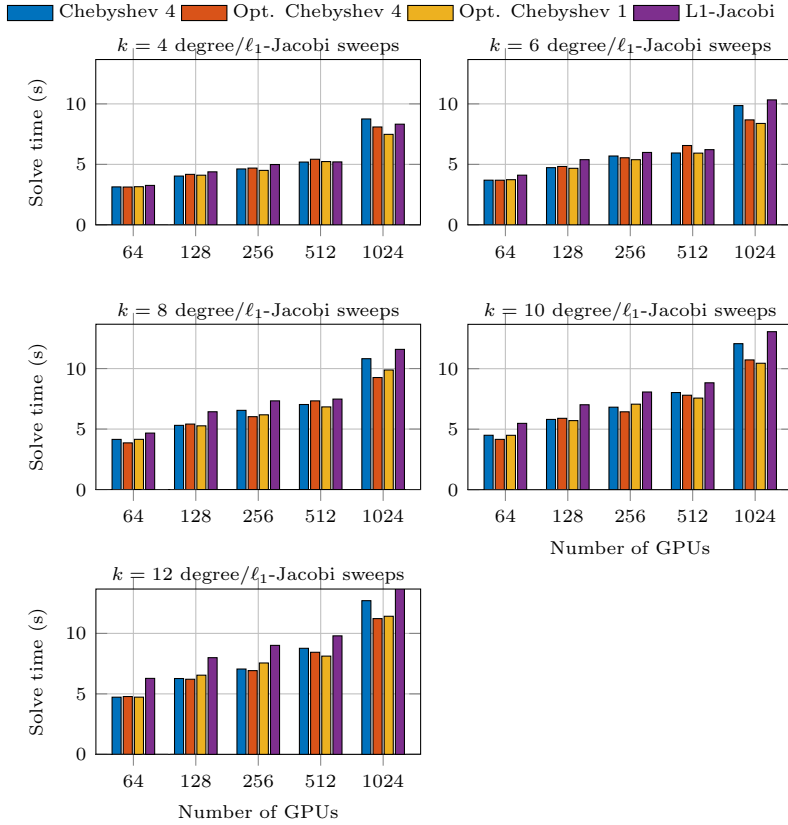


Fig. 15: Solve time (s). Time to solution (s) for the Poisson 3D test case employing the multigrid scheme based on the VBM aggregation in conjunction with the different polynomial accelerators and the baseline ℓ_1 -Jacobi for comparison.

the same code on the CPU or GPU by changing only the allocation type, `PSCToolkit` exploits the Fortran `MOLD` option and a dynamic data type management. The `MOLD` option in Fortran is routinely used in the `ALLOCATE` statements to create a new array or scalar variable that has the same type and type parameters as an existing array or scalar. We have adapted the same mechanism to work with the distributed matrix and vector data formats in `PSBLAS`. For the examples in Section 4 we have used the GPU version of the Ellpack format, this can be achieved by instantiating the pointer variables:

```
type(psb_d_cuda_hlg_sparse_mat), target :: ahlg
type(psb_d_vect_cuda), target          :: dvgpu
type(psb_i_vect_cuda), target          :: ivgpu
```

and pass them in the assembly phases of the matrix, descriptor and vector objects so that they are instantiated and built on the device,

```
call psb_cdasb(desc, info, mold=ivgpu)
call psb_spasb(a, desc, info, mold=ahlg)
call psb_geasb(b, desc, info, mold=dvgpu)
```

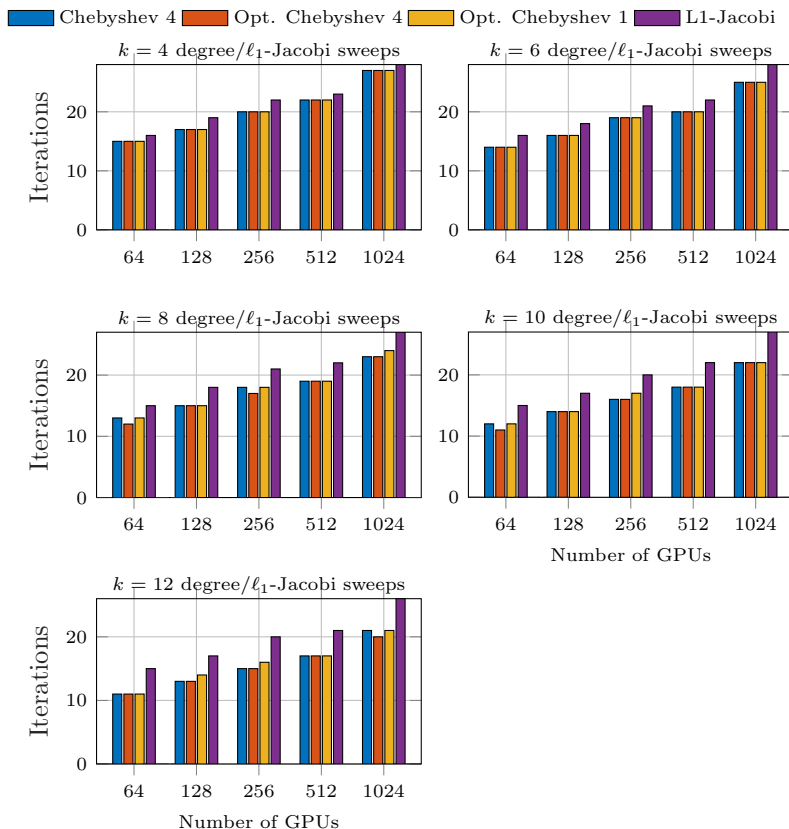


Fig. 16: Iteration count. Total number of FCG iterations for the Poisson 3D test case employing the multigrid scheme based on the VBM aggregation in conjunction with the different polynomial accelerators and the baseline ℓ_1 -Jacobi for comparison.

where `a`, `b` and `desc` are the sparse matrix A , the right-hand side \mathbf{b} and the descriptor respectively. Setting and constructing the AMG preconditioners on the matrix A is equally easy. This is an object of type

```
type(amg_dprec_type) :: prec
```

and after being declared, and the assembly of the matrix A (`call psb_spasb()`), can have options set with the following calls:

```
call prec%init(ctxt, 'ML', info)
call prec%set('ml_cycle', 'V-Cycle', info)
call prec%set('outer_sweeps', 1, info)
call prec%set('aggr_prol', 'COUPLED', info)
call prec%set('par_aggr_alg', 'MATCHBOXP', info)
call prec%set('aggr_type', 'SMOOTHED', info)
call prec%set('aggr_size', 8, info)
call prec%set('smoother_type', 'POLY', info)
call prec%set('poly_degree', 5, info)
call prec%set('poly_variant', 'CHEB_1_OPT', info)
call prec%set('coarse_solve', 'L1-JACOBI', info)
```

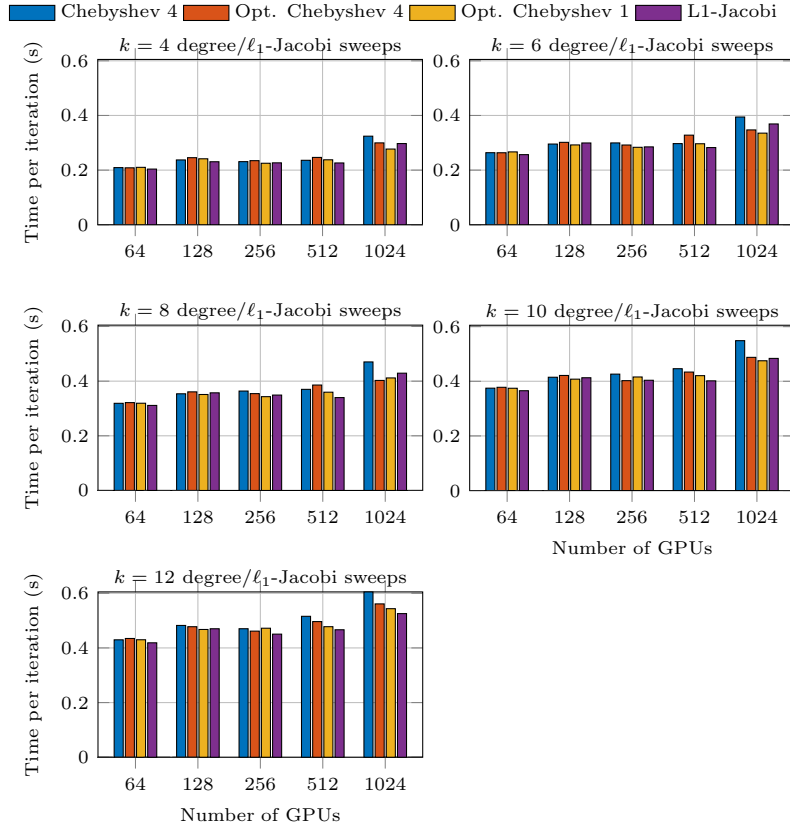


Fig. 17: Time per iteration. Time per iteration for the Poisson 3D test case employing the multigrid scheme based on the VBM aggregation in conjunction with the different polynomial accelerators and the baseline ℓ_1 -Jacobi for comparison.

```
call prec%set('coarse_mat','DIST',info)
call prec%set('coarse_sweeps',30,info)
```

This set of calls sets up the V-cycle-based AMG preconditioner, which uses the matching-based aggregation scheme compatible with aggregates of size at most 8. The smoother is the polynomial one based on Chebyshev polynomials of the 1st-kind and degree 5. The ℓ_1 -Jacobi method is used to solve the coarsest system (30 iterations).

Once we are satisfied with the algorithmic choices made we can ask for the assembly of the preconditioner, an operation that is done in two separate parts, one for the hierarchy and one for the smoothers and also ask to pre-allocate the work vectors on the device:

```
call prec%hierarchy_build(a,desc,info)
call prec%smoothers_build(a,desc,info,amold=ahlg,vmold=dvgpu, &
& imold=ivgpu)
call prec%allocate_wrk(info,vmold=dvgpu)
```

Note that in general it is possible to reuse the same hierarchy with different smoothers, so if you change your mind—or want to try a different smoother with the same hierarchy—it is sufficient to make the appropriate set calls and call the function

SM8 P. D'AMBRA, F. DURASTANTE, S. FILIPPONE, S. MASSEI, AND S. THOMAS.

```
prec%smoothers_build( ).
```

The solution employing the Flexible Conjugate Gradient can then be obtained by the call

```
call psb_krylov('FCG',a,prec,b,xvec,1d-7,desc,info,itmax=100,itrace=1)
```

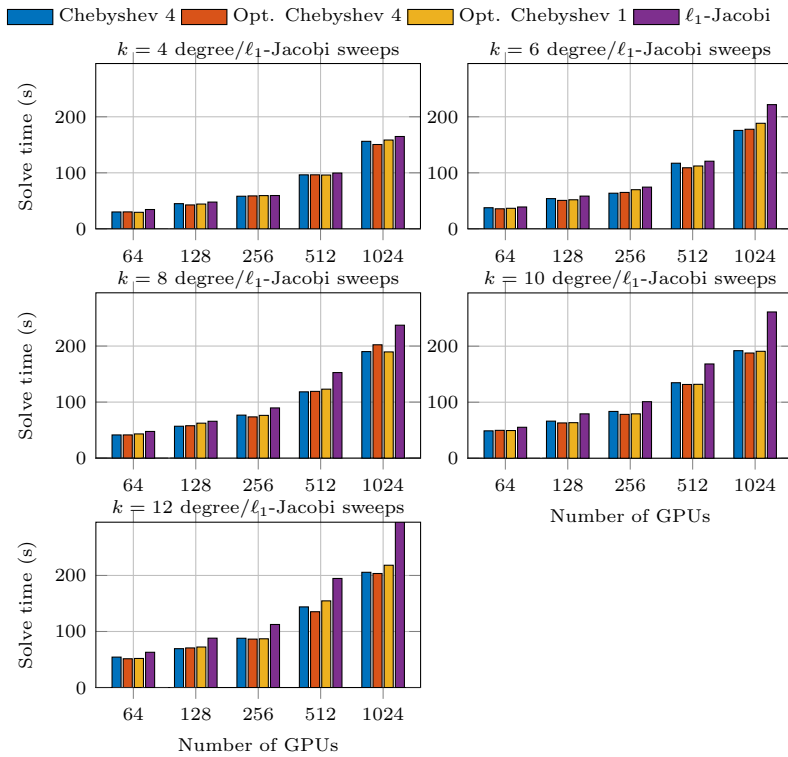


Fig. 18: Solve time (s). Time to solution (s) for the Anisotropy 2D test case ($\varepsilon = 100, \theta = \pi/6$) employing the multigrid scheme based on the VBM aggregation in conjunction with the different polynomial accelerators and the baseline ℓ_1 -Jacobi for comparison.

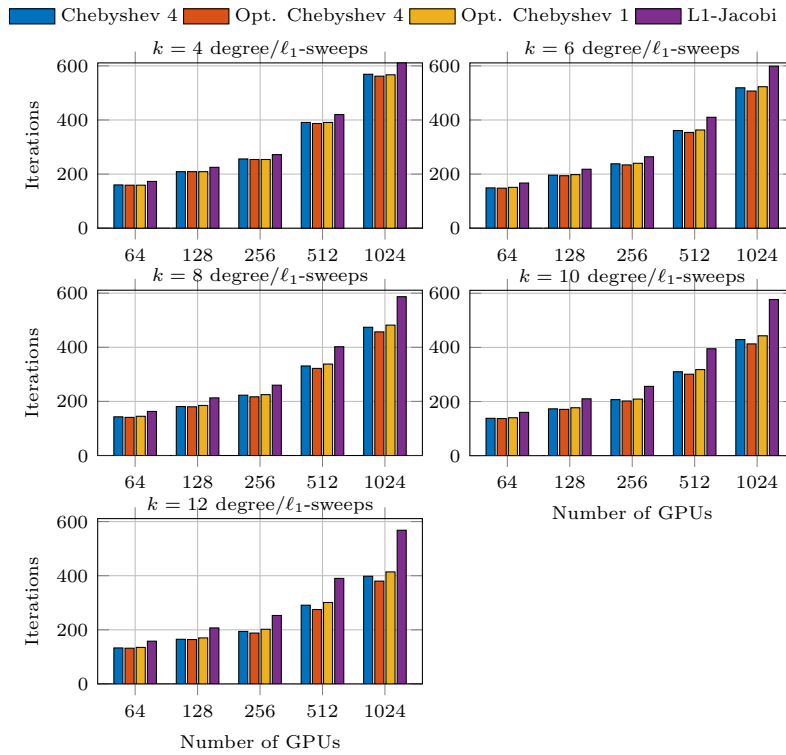


Fig. 19: Iteration count. Total number of FCG iterations for the Anisotropy 2D test case ($\varepsilon = 100, \theta = \pi/6$) employing the multigrid scheme based on the VBM aggregation in conjunction with the different polynomial accelerators and the baseline ℓ_1 -Jacobi for comparison.

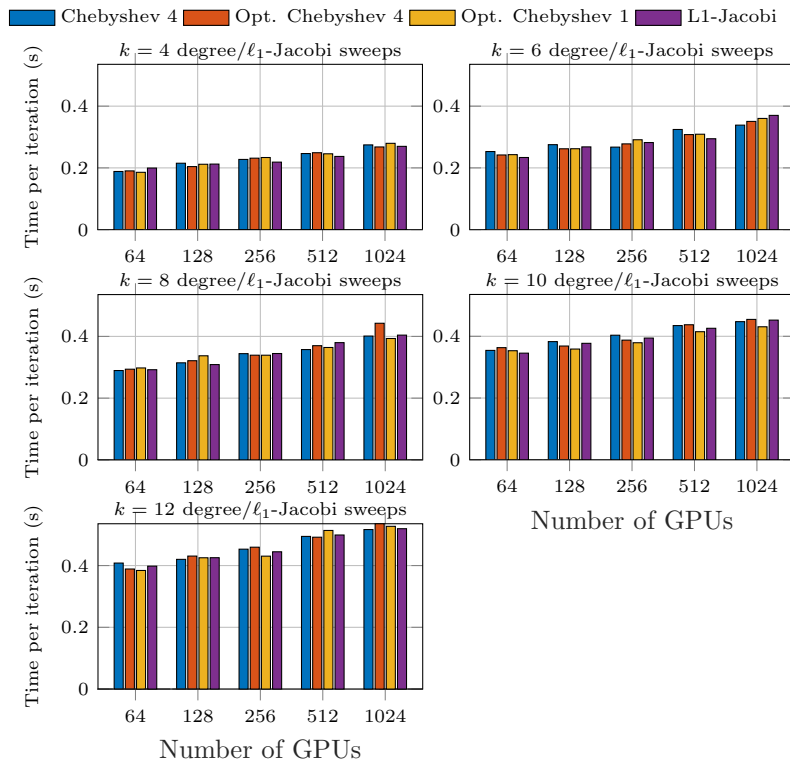


Fig. 20: Time per iteration. Time per iteration for the Anisotropy 2D test case ($\varepsilon = 100, \theta = \pi/6$) employing the multigrid scheme based on the VBM aggregation in conjunction with the different polynomial accelerators and the baseline ℓ_1 -Jacobi for comparison.

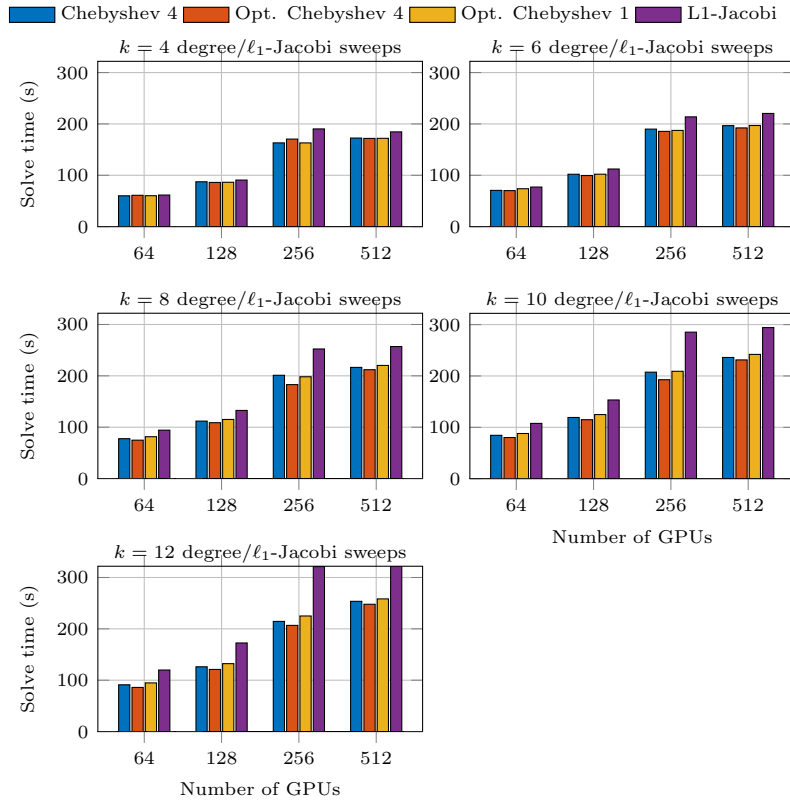


Fig. 21: Solve time (s). Time to solution (s) for the Anisotropy 2D test case ($\varepsilon = 100, \theta = \pi/6$) employing the multigrid scheme based on the compatible matching aggregation in conjunction with the different polynomial accelerators and the baseline ℓ_1 -Jacobi for comparison.

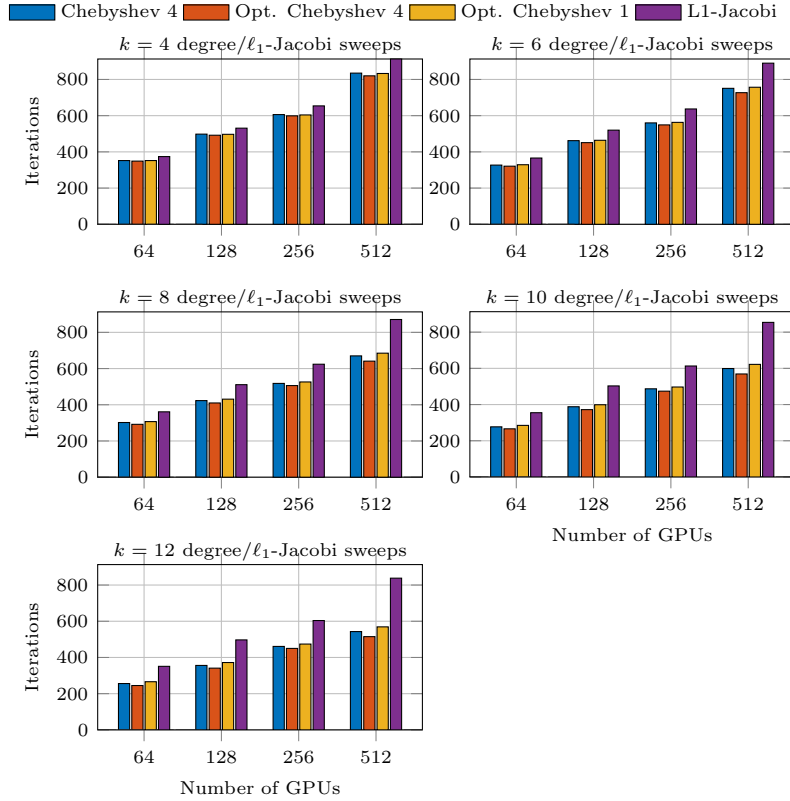


Fig. 22: Iteration count. Total number of FCG iterations for the Anisotropy 2D test case ($\varepsilon = 100, \theta = \pi/6$) employing the multigrid scheme based on the compatible matching aggregation in conjunction with the different polynomial accelerators and the baseline ℓ_1 -Jacobi for comparison.

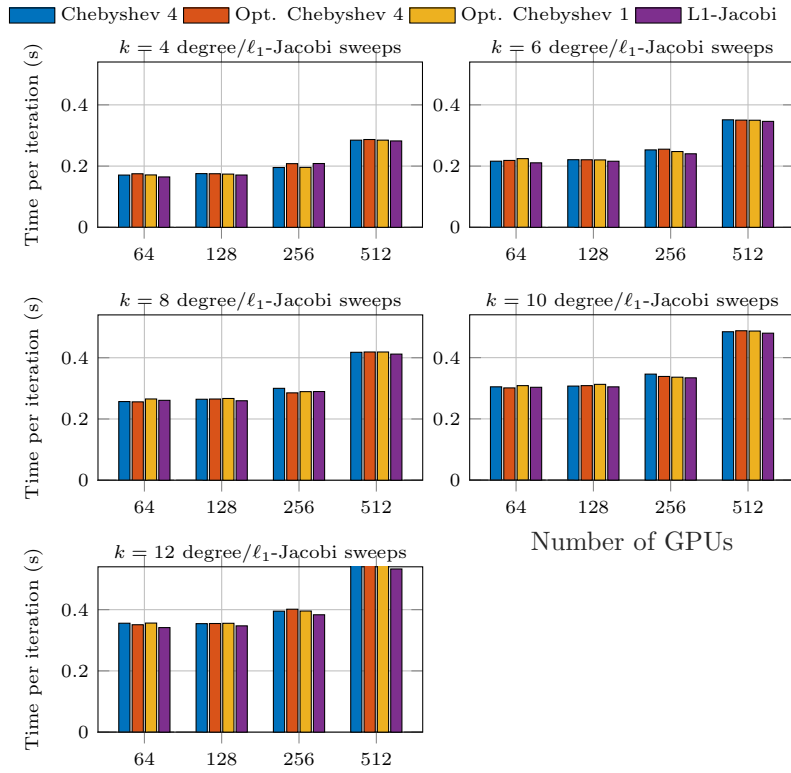


Fig. 23: Time per iteration. Time per iteration for the Anisotropy 2D test case ($\varepsilon = 100, \theta = \pi/6$) employing the multigrid scheme based on the compatible matching aggregation in conjunction with the different polynomial accelerators and the baseline ℓ_1 -Jacobi for comparison.